UCL

CARNEGIE INSTITUTION FOR SCIENCE

Quantum Monte Carlo simulations on silicate perovskite and other high pressure phases

R E Cohen[1,2]

[1]Geophysical Laboratory, Carnegie Institution
[2]Dept. Earth Science, University College London

Funded by NSF and ERC

DFT, QMC, and DFT-DMFT Studies of some high pressure materials

- SiO_2 (CASINO) (Driver, Cohen, Wu, Militzer, Rios, Towler, Needs, & Wilkins, *PNAS* **107**, 9519 (2010).
- qmcpack on GPUs (Esler, Kim, Ceperley)
- c-BN (qmcpack, GPU)(Esler, Cohen, Militzer, Kim, Needs, & Towler, PRL **104**, 185702 (2010).
- $MgSiO_3$ (qmcpack, GPU) (Lin et al., submitted)
- $FeSiO_3$ (DFT, xtalopt)(Cohen and Lin, submitted)
- FeO (DFT-DMFT) (Ohta, Cohen, Hirose, Haule, Shimizu & Ohishi, PRL**108**, 026403, (2012)

Beyond DFT: Quantum Monte Carlo

Benchmark computations as standard

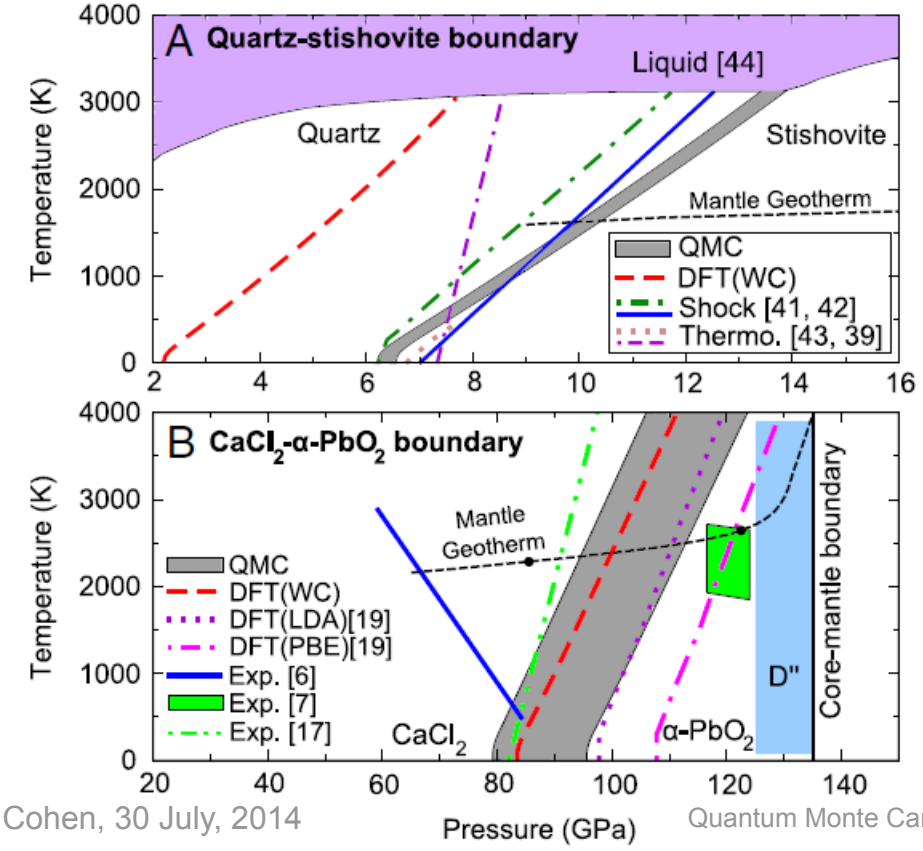

Boundary between Quartz and stishovite phases of SiO_2

Boundary between $CaCl_2$ and α-PbO_2 phases of SiO_2

K. P. Driver, R. E. Cohen, Z. Wu, B. Militzer, et al., *PNAS*, 107, 9519-9524 (2010)

Ken Esler (GL, Stone Ridge Technologies) Jeongnim Kim (NCSA, ORNL, Intel), Dave Ceperley (UIUC)

- Ported the main functionality of a major QMC code to run fully on GPU clusters
- In use for production simulations
  - e.g. Phys. Rev. Lett. 104, 185702 (2010)
- Achieves about 15x quad-core processor
  - Some caveats (e.g. mixed precision vs. double
  - CPU code is well optimized (SSE intrinsics, etc.)
- Parallelized to run on MPI clusters of GPUs
  - ~88% parallel efficiency with 256 GPUs

Why QMC on GPUs?

- QMC consumes many cycles
  - e.g. ~70 million core hours on Jaguar in 2009
  - 8k cores 24/7
- It affords multiple levels for parallelization
  - "Natural" Monte Carlo parallelism (walkers)
  - Electrons, orbitals, ions, etc.
- MPI communication requirements are low
  - Primarily for load balancing
- With GPUs
  - Small problems are doable on a workstation
  - Large problems are much cheaper

Why not QMC on GPUs?

- Many kernels to port
  - No single major kernel
  - Wave functions take many forms
  - Subset of functionality:
  - ~100 CUDA kernels, ~10k lines of kernel code
- Algorithms and data need restructuring
  - Need to utilize more parallelism than on CPUs
- Debugging stochastic methods is hard
- No libraries for the kernels we need

QMCPACK

- http://www.qmcpack.org
  - Paul Kent, ORNL (was Jeongnim Kim)
- https://groups.google.com/forum/#!forum/qmcpack
- Open source C++ code (NCSA license)
- Hybrid OpenMP/MPI programming model
  - Scaled to > 200k cores with > 90% efficiency
- Heavy use of template meta-programming
  - At least as fast as any comparable code
  - Kernels hand-tuned with SSE
- Object-oriented style for extensibility

QMCPACK

- Variational Monte Carlo
- Diffusion Monte Carlo
- Reptation
- Single and multi-determinant Slater Jastrow wavefunctions
- Wavefunction updates using optimized multi-determinant algorithm of Clark et al.
- Backflow wavefunctions
- One, two, and three-body Jastrow factors
- Excited state calculations via flexible occupancy assignment of Slater determinants
- All electron and non-local pseudopotential calculations
- Casula T-moves for variational evaluation of non-local pseudopotentials
- Wavefunction optimization using the “linear method” of Umrigar and co-workers, with arbitrary mix of variance and energy in the objective function
- Gaussian, Slater, plane-wave and real-space spline basis sets for orbitals
- Interface and conversion utilities for plane-wave wavefunctions from Quantum Espresso (PWSCF)
- Interface and conversion utilities for Gaussian-basis wavefunctions from GAMESS
- Easy extension and interfacing to other electronic structure codes via standardized XML and HDF5 inputs
- MPI parallelism
- Fully threaded using OpenMP
- GPU (CUDA) implementation (limited functionality)
- HDF5 input/output for large data
- “Project Suite” advanced workflow tool to automate all aspects of QMC calculation from initial DFT calculations through to final analysis
- Analysis tools for minimal environments (perl only) through to python-based with graphs produced via matplotlib.
- Although primarily used for electronic structure problems, within QMCPACK the Hamiltonian definition is very flexible and also suited to some model systems.

- K. Esler, J. Kim, L. Shulenburger, and D. Ceperley, "Fully accelerating quantum Monte Carlo simulations of real materials on GPU clusters", *Computing in Science and Engineering* doi: 10.1109/MCSE.2010.122 (2010)
- Symposium on Application Accelerators in High Performance Computing http://saahpc.ncsa.illinois.edu/10/papers/paper_27.pdf
- K. P. Esler, R. E. Cohen, B. Militzer, Jeongnim Kim, R. J. Needs, and M. D. Towler, "Fundamental High-Pressure Calibration from All-Electron Quantum Monte Carlo Calculations", Phys. Rev. Lett. 104, 185702 (2010)

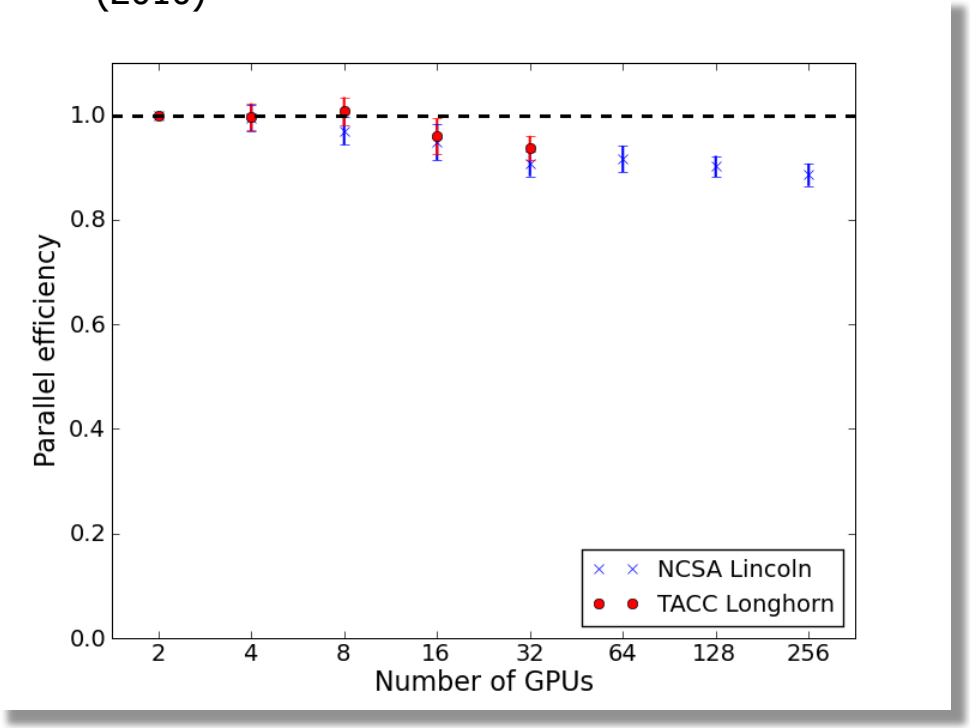

- Higher throughput on GPUs puts greater demand on interconnect
- Down to 88% efficiency on Lincoln at 256 GPUs
- Newer clusters have faster interconnects and PCI-E bus
  (e.g. upcoming Cray XK6)
- Direct GPU-to-GPU transfer now possible on one node

cBN as a pressure standard

Cubic boron nitride is an ideal pressure standard.

- Stable over wide pressure and temperature range
- Single Raman mode for calibration
- Single lattice parameter

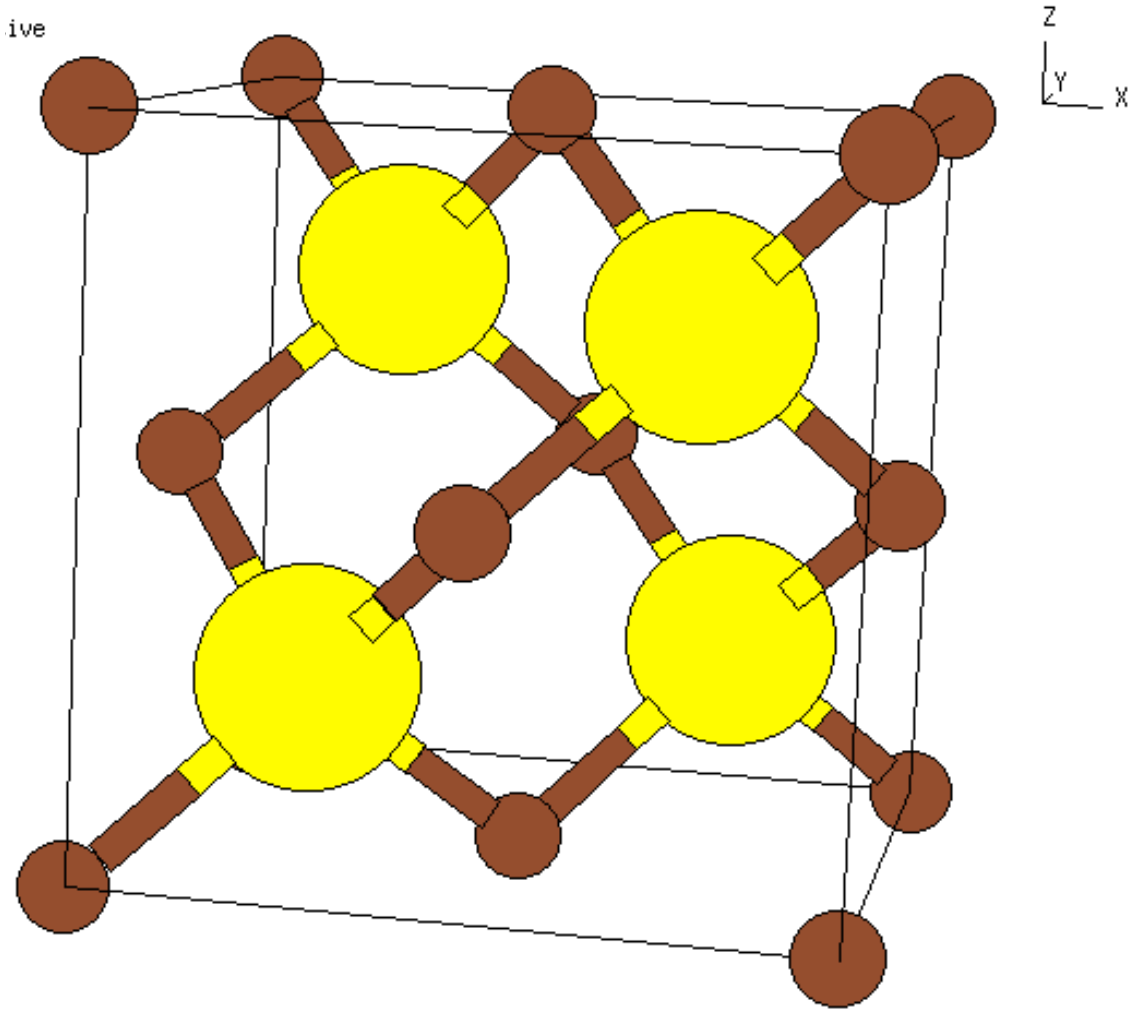

Equation of state of c-BN

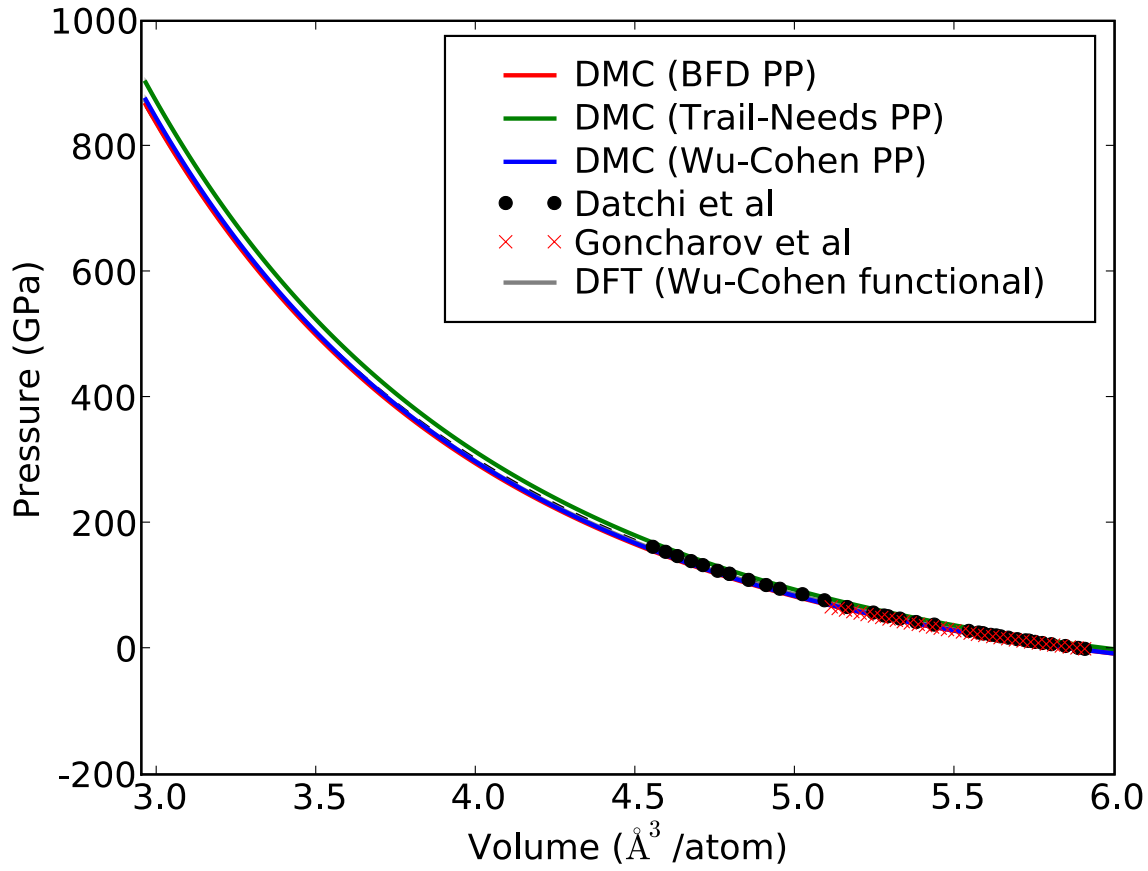

Equation of state of c-BN: comparing PPs

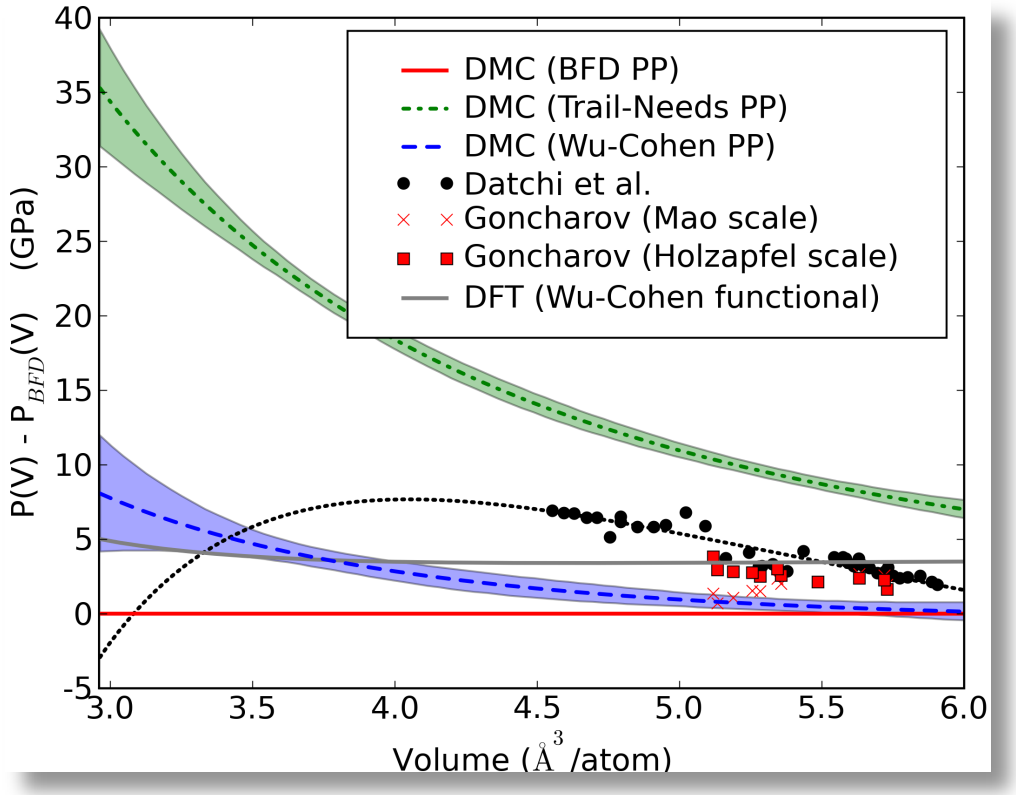

About a 5% discrepancy at high pressure:
not useful for an *ab initio* calibration!

All-electron QMC for solids

- Current QMC calculations on solids use pseudopotentials (PPs) from Hartree-Fock or DFT
- When different PPs give different results, how do we know which to use?
- In DFT, decide based on agreement with all-electron calculation
- We would like to do the same in QMC. Has only been done for hydrogen and helium.

- LAPW is generally gold standard for DFT.
- Use orbitals from LAPW calculation in QMC simulation.
- Requires efficient evaluation methods and careful numerics
- Use atomic-like representation near nuclei, plane-wave or B-splines in interstitial region:

$$\phi_{n,\mathbf{k}}(\mathbf{r}) = \begin{cases} \sum_{\mathbf{G}} \sum_{l,m,j} c_{n,\mathbf{G}+\mathbf{k}} A^{\alpha}_{j,l,m} u^{\alpha}_{j,l}(r) Y_{lm}(\hat{\mathbf{r}}) & \text{if } \mathbf{r} \in \text{muffin tin} \\ \Omega^{-\frac{1}{2}} \sum_{\mathbf{G}} c_{n,\mathbf{G}+\mathbf{k}} e^{i(\mathbf{G}+\mathbf{k})\cdot\mathbf{r}} & \text{otherwise} \end{cases}$$

Results

- After all-electron correction, EOS from 3 PPs in perfect agreement
- Details in EPAS of Phys. Rev. Lett. 104, 185702 (2010)

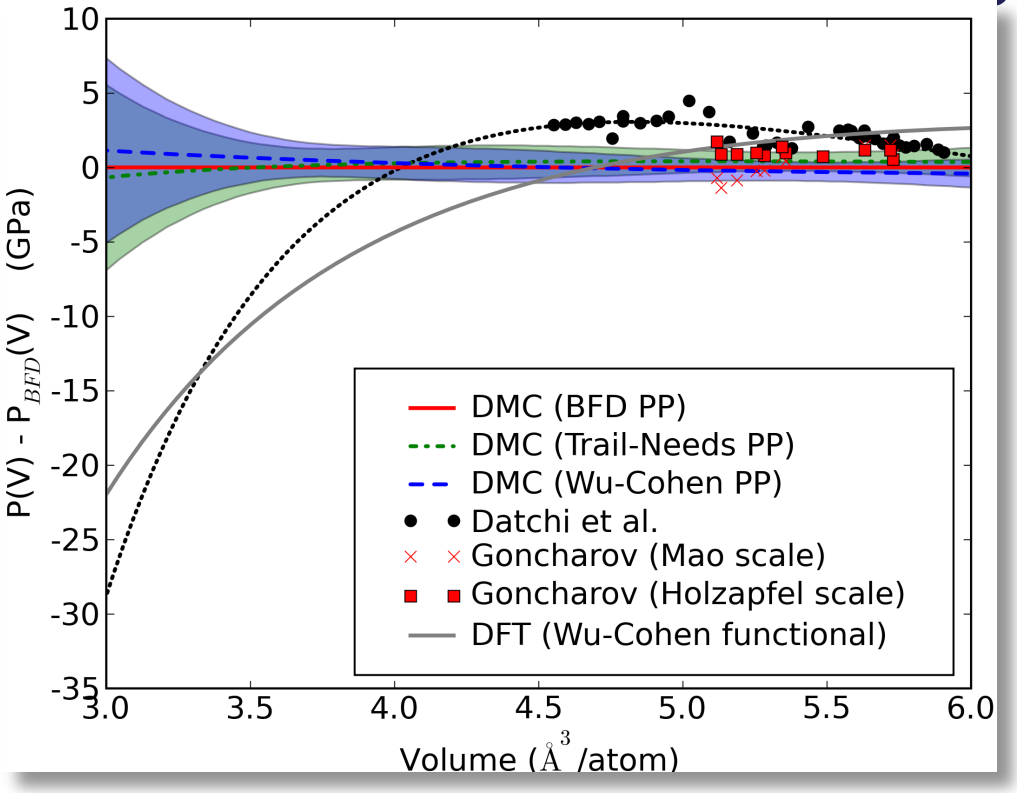

cBN Raman Frequencies

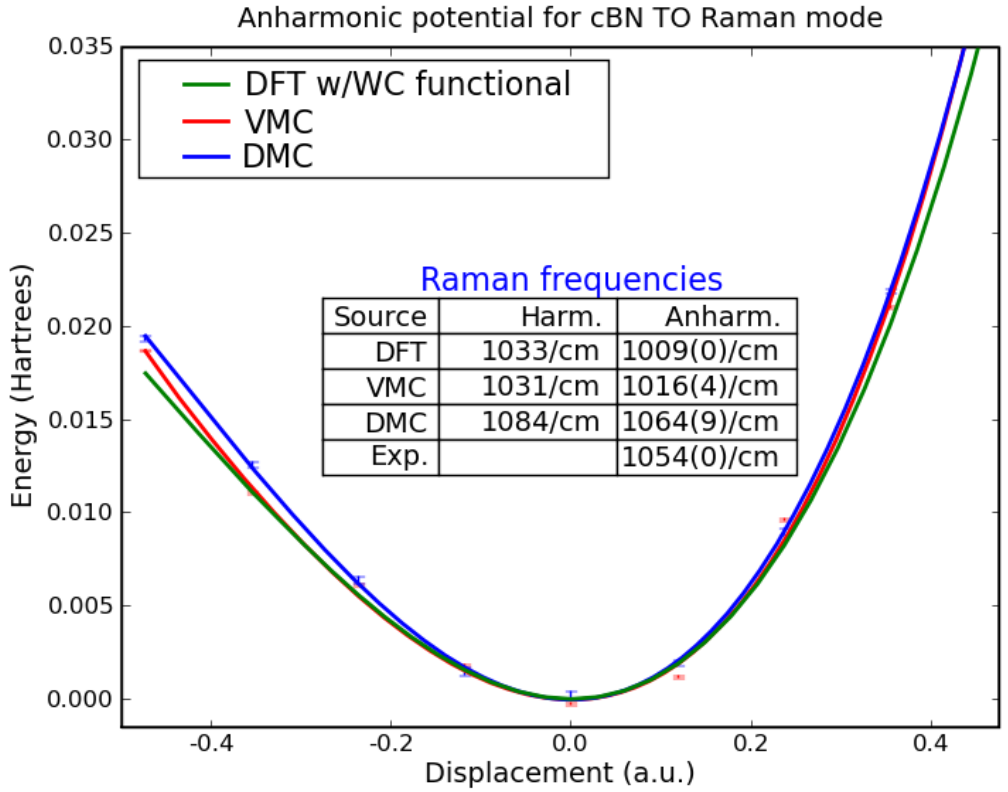

Raman frequencies

Source	Harm.	Anharm.
DFT	1033/cm	1009(0)/cm
VMC	1031/cm	1016(4)/cm
DMC	1084/cm	1064(9)/cm
Exp.		1054(0)/cm

- Within harmonic approx. DFT frequency is reasonable
- But, cBN Raman mode is quite anharmonic
- With anharmonic corrections, DFT frequencies are not so good.
- Compute energy vs. displacement with DMC and do 4th-order fit. Solve 1D Schrodinger eq. to get frequency
- Anharmonic DMC frequency is correct to within statistical error

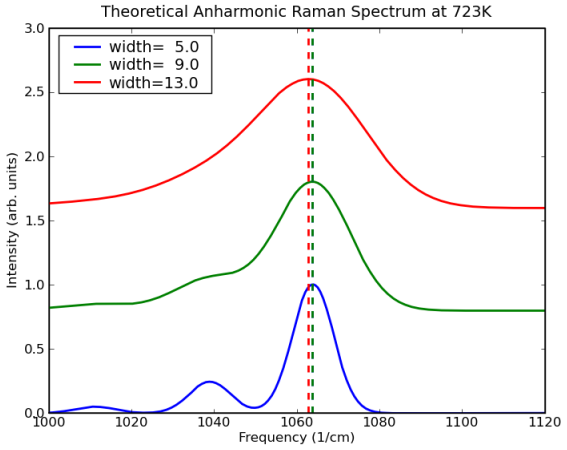

cBN Raman Frequencies

- Raman frequencies are linear in 1/V
- When combined with EOS, data can be used to directly measure pressure from the Raman frequency
- There is some intrinsic T-dependent shift due to anharmonicity

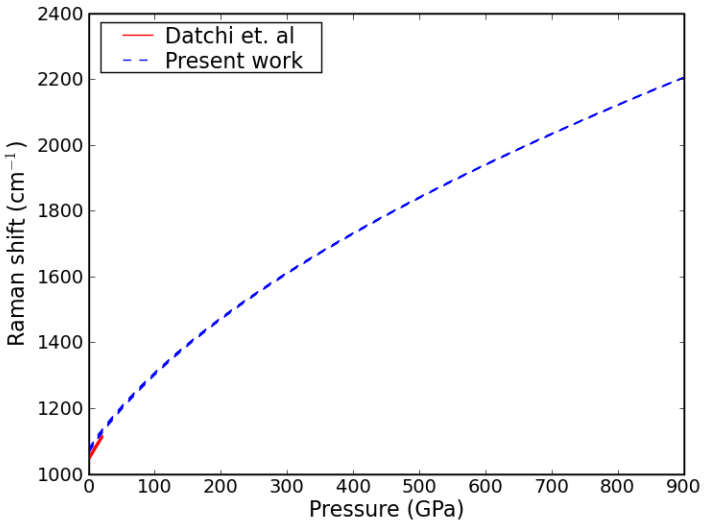

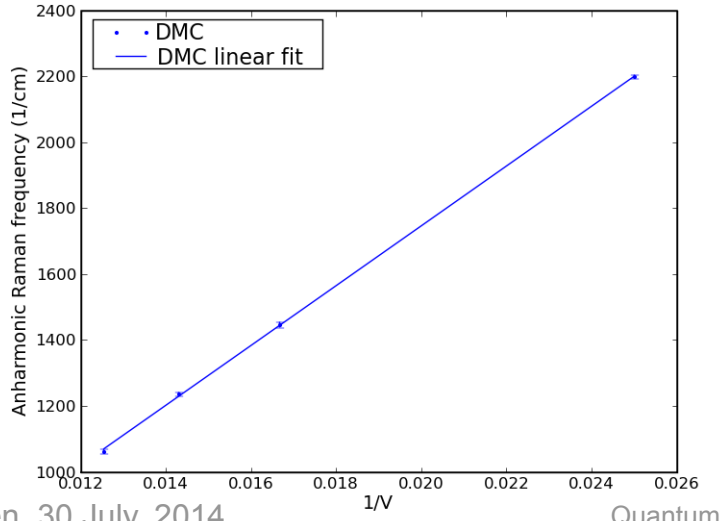

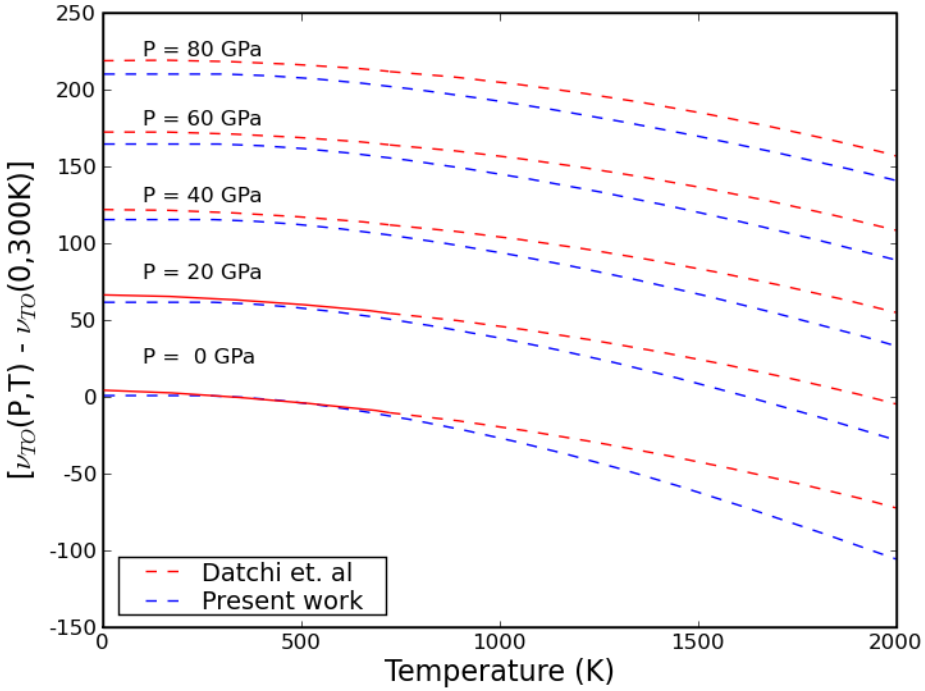

MgSiO3, the Dominant Component of the Earth's Lower Mantle

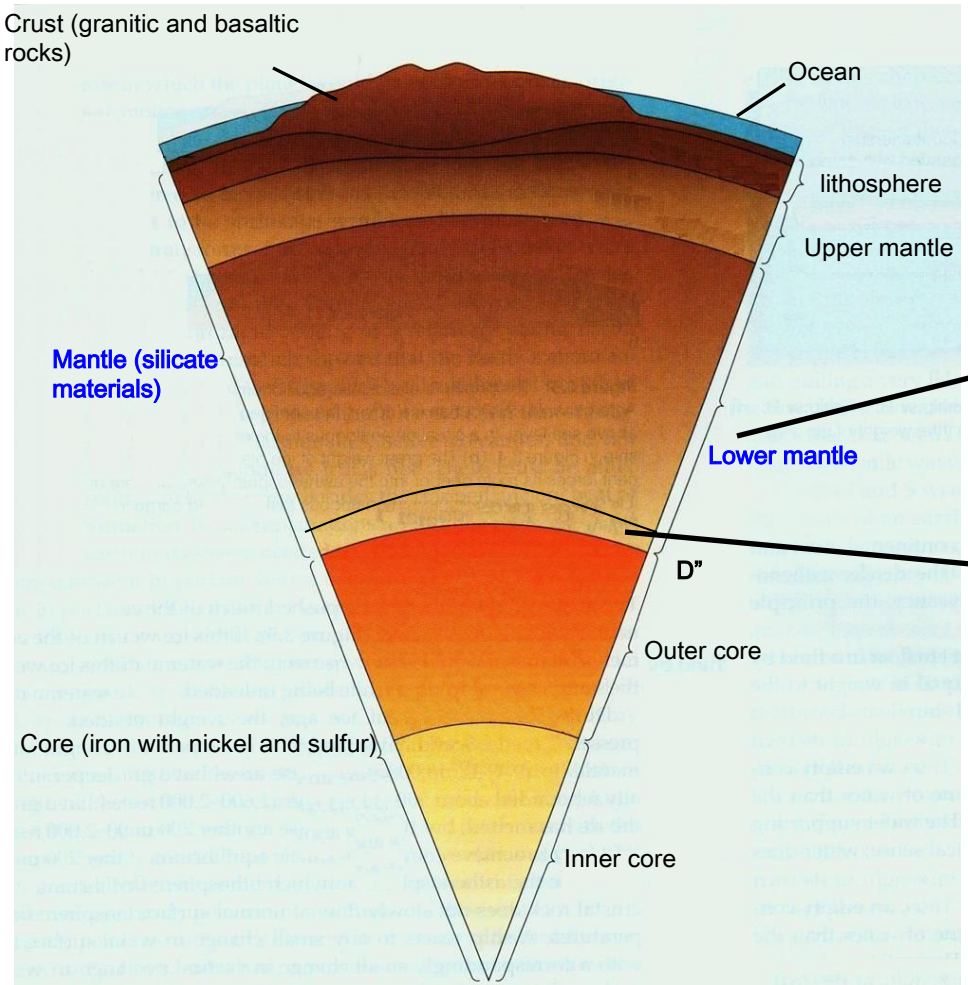

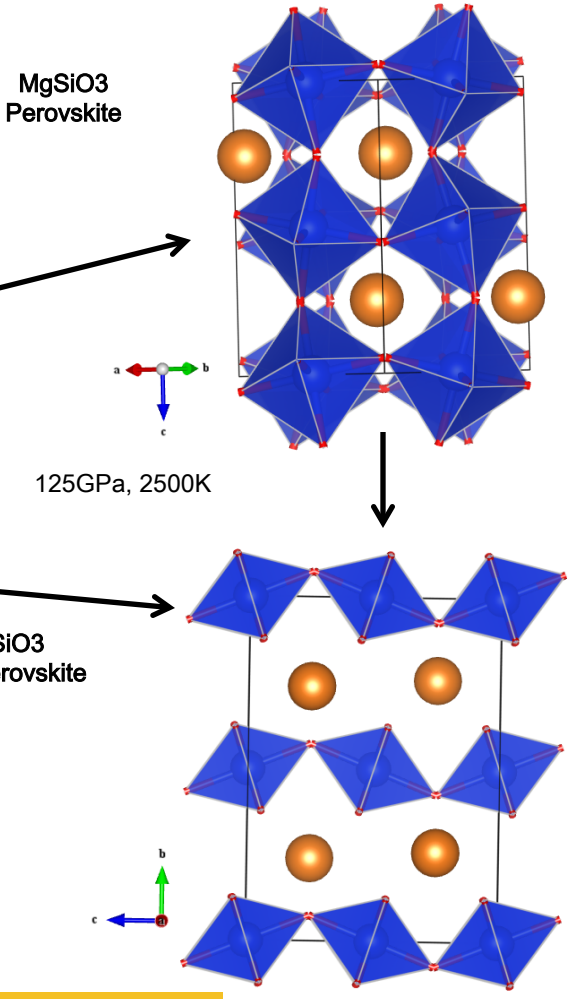

M. Murakami, K. Hirose, K. Kawamura, et al., *Science*, 304, 855-858 (2004)
T. Litaka, K. Hirose, K. Kawamura, et al., *Nature*, 430, 442-445 (2004)

SCIENCE, VOL. 235

1987

Reports

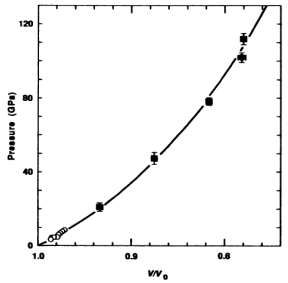

Synthesis and Equation of State of $(Mg,Fe)SiO_3$ Perovskite to Over 100 Gigapascals

ELISE KNITTLE AND RAYMOND JEANLOZ

Silicate perovskite of composition $(Mg_{0.88}Fe_{0.12})SiO_3$ has been synthesized in a laser-heated diamond-anvil cell to a pressure of 127 gigapascals at temperatures exceeding 2000 K. The perovskite phase was identified and its unit-cell dimensions measured by in situ x-ray diffraction at elevated pressure and room temperature. An analysis of these data yields the first high-precision equation of state for this mineral, with values of the zero-pressure isothermal bulk modulus and its pressure derivative being K_{0T} = 266 ± 6 gigapascals and K'_{0T} = 3.9 ± 0.4. In addition, the orthorhombic distortion of the silicate-perovskite structure away from ideal cubic symmetry remains constant with pressure: the lattice parameter ratios are b/a = 1.032 ± 0.002 and c/a = 1.444 ± 0.006. These results, which prove that silicate perovskite is stable to ultrahigh pressures, demonstrate that perovskite can exist throughout the pressure range of the lower mantle and that it is therefore likely to be the most abundant mineral in Earth.

Equations of state and stability of $MgSiO_3$ perovskite and post-perovskite phases from quantum Monte Carlo simulations

Yangzheng Lin[1], R. E. Cohen[1,2],* Stephen Stackhouse[3,5], Kevin P. Driver[3], Burkhard Militzer[3,4], Luke Shulenburger[6], and Jeongnim Kim[7]

[1] *Geophysical Laboratory, Carnegie Institution of Washington, 5251 Broad Branch Road, NW, Washington DC 20015, USA*

[2] *Department of Earth Science, University College London, UK*

[3] *Departments of Earth and Planetary Science and* [4] *of Astronomy, University of California, Berkeley, CA 94720, USA*

[5] *School of Earth and Environment, University of Leeds, Leeds, UK*

[6] *Sandia National Laboratories, Albuquerque, NM, USA and*

[7] *Oak Ridge National Laboratory, Oak Ridge, TN, USA*

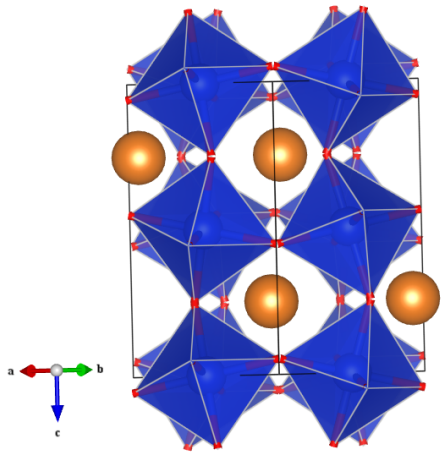

$MgSiO_3$ Perovskite

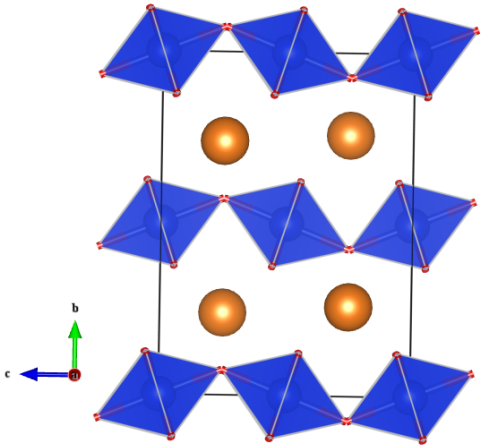

$MgSiO_3$ Post-Perovskite

Supported by NSF

QMC computations for $MgSiO_3$ perovskite and post-perovskite

https://code.google.com/p/qmcpack/

We obtained the QMC trial wavefunction from DFT calculations using PWSCF

$$\psi_{\mathrm{AS}} = \sum_i C_i D_i^{\uparrow}(\phi) D_i^{\downarrow}(\phi)$$

$\{\phi\}$ denotes a set of single-particle orbitals. $D^{\uparrow}\left(D^{\downarrow}\right)$ are the up-(down-) spin Slater determinant.

We obtained the optimized one and two-body Jastrow factors using VMC calculations with a linear method

$$\psi_{\mathrm{T}} = J_1 J_2 \psi_{\mathrm{AS}}$$

$$J_1 = \exp\left[\sum_I^{ion0}\sum_i^{e} u_{ab}\left(|\mathbf{r}_i - \mathbf{R}_I|\right)\right]$$

$$J_2 = \exp\left[\sum_i^{e}\sum_j^{e} u_{ab}\left(|\mathbf{r}_i - \mathbf{r}_j|\right)\right]$$

A better set of Jastrow factors gives the smaller VMC energy and lower variance

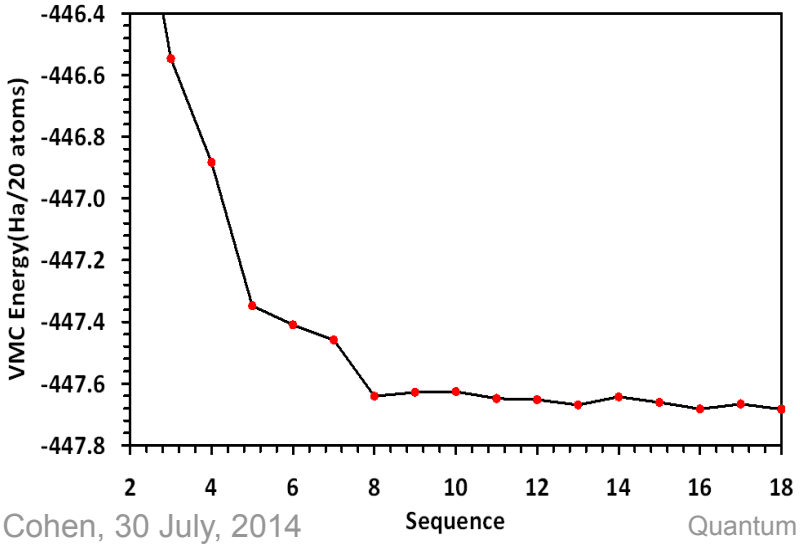

We obtained the total energies using DMC calculations with 0.001 steptime and 25,000 steps

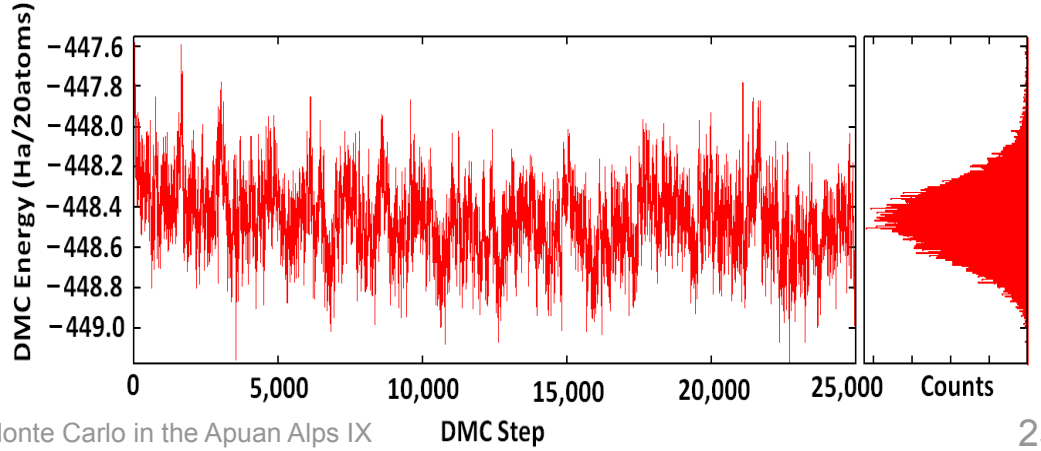

Finite Size Corrections and Infinite Size Energy Extrapolation

QMC deals with isolated systems and without consideration of periodic boundary conditions

We used the 8 twists average to reduce the one-body finite size errors. To reduce the two-body finite size errors, we used the Model Periodic Coulomb (MPC) interaction to correct the potential energy and used the scheme of Chiesa, Ceperley and Martin (CCM) to correct the kinetic energy.

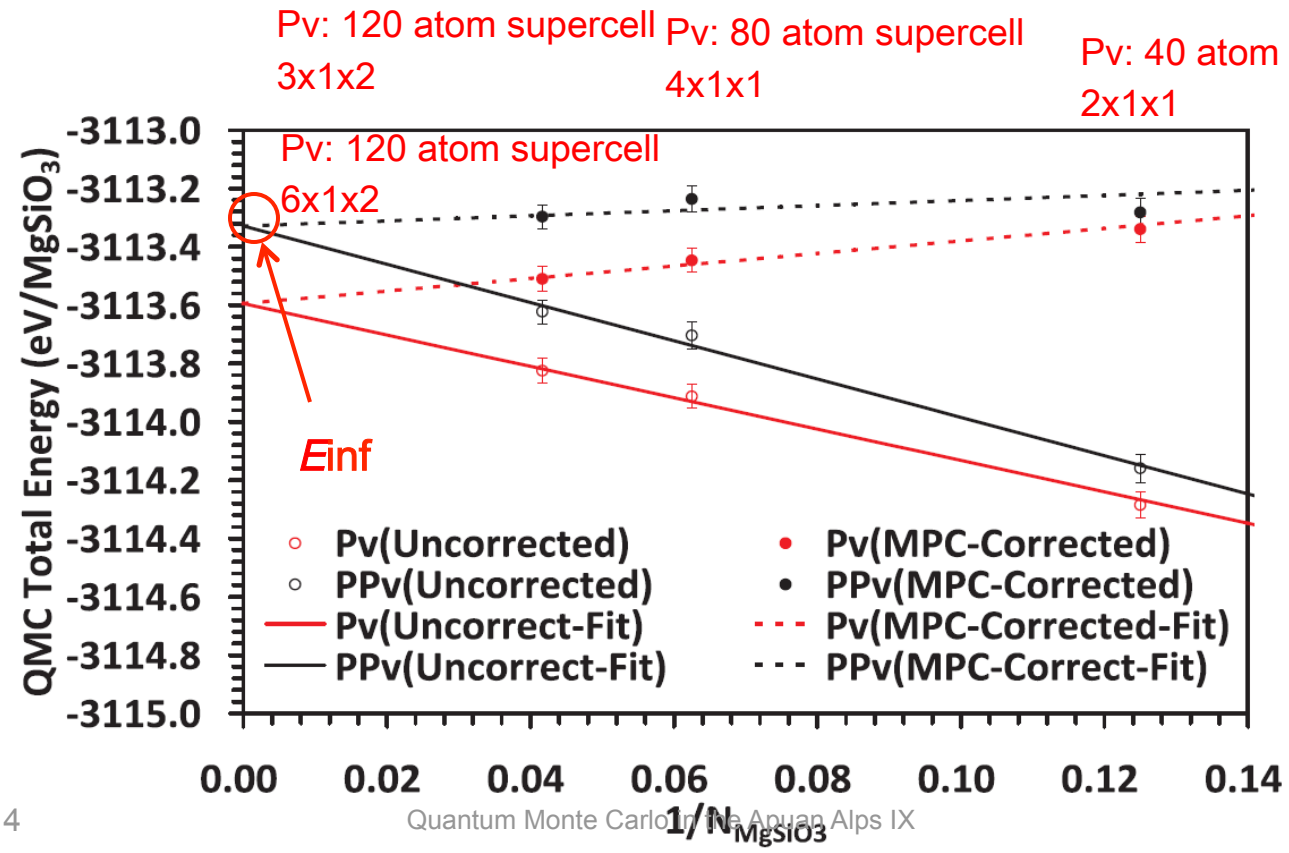

QMC Equations of States of MgSiO3 Perovskite and Post-Perovskite

With the above procedures, we obtained the DFT and DMC energies at several volumes of MgSiO3 Perovskite and Post-Perovskite cells

Vinet energy and pressure equations

$$E = E_0 + \frac{4K_0V_0}{(K_0'-1)^2} - 2V_0K_0(K_0'-1)^{-2}\left[5+3K_0'(x-1)-3x\right]\exp\left[-\frac{3}{2}(K_0'-1)(x-1)\right]$$

$$P = \left[\frac{3K_0(1-x)}{x^2}\right]\exp\left[-\frac{3}{2}(K_0'-1)(x-1)\right] \qquad x = (V/V_0)^{1/3} \qquad H = E + PV$$

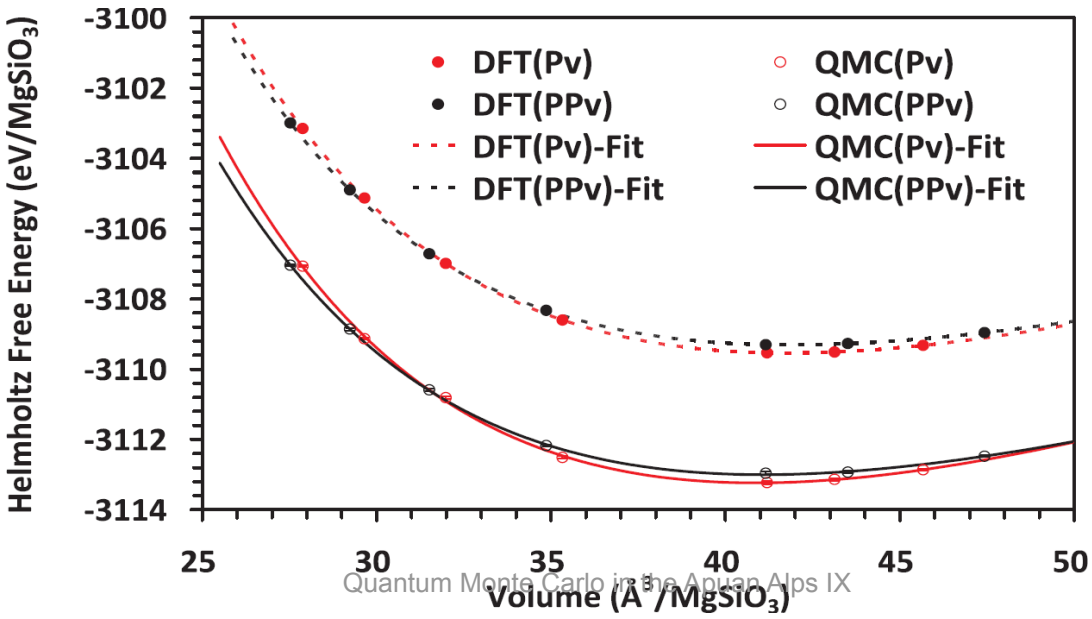

Thermal Equation of State Parameters, Pv

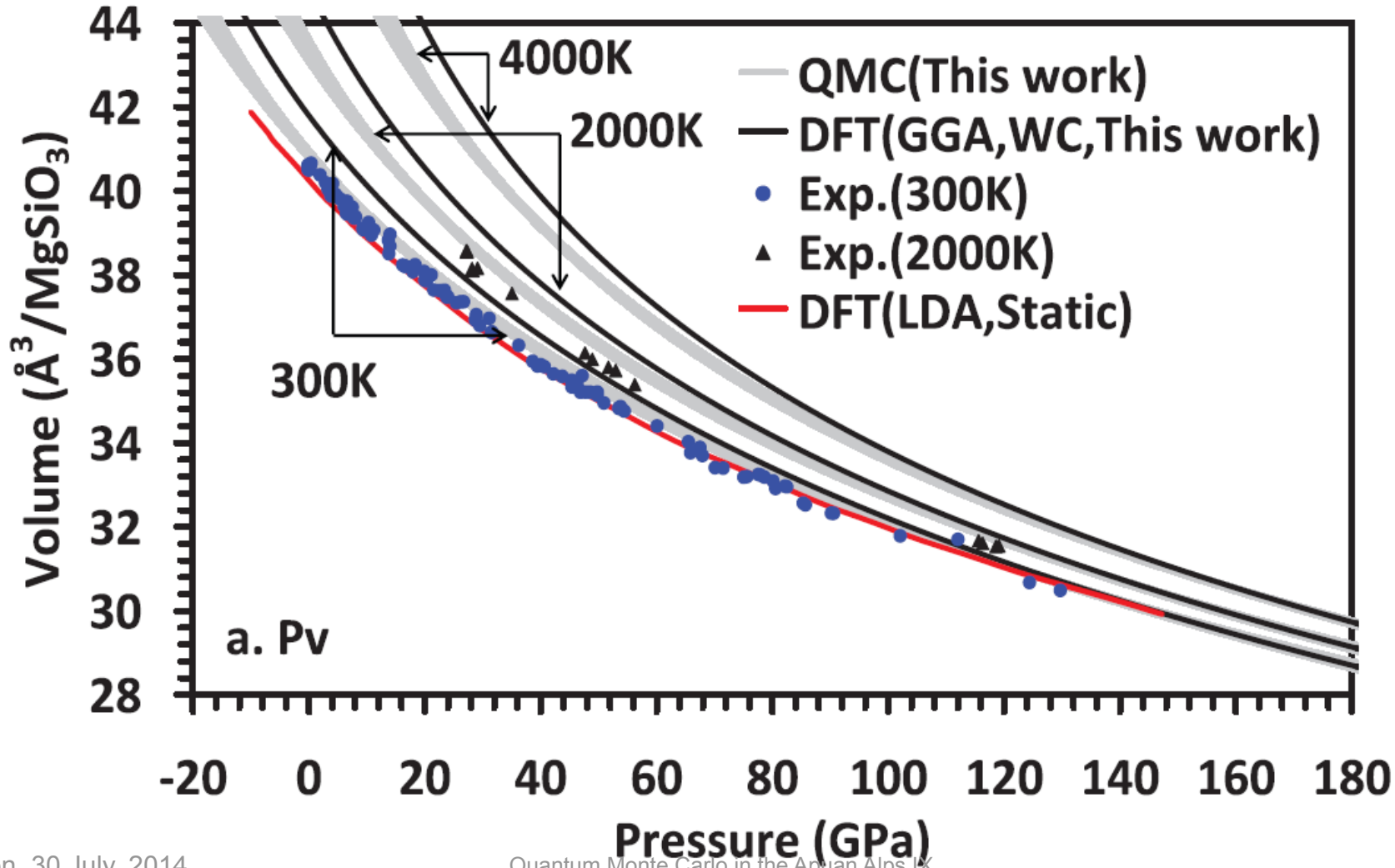

Thermal Equation of State Parameters, PPv

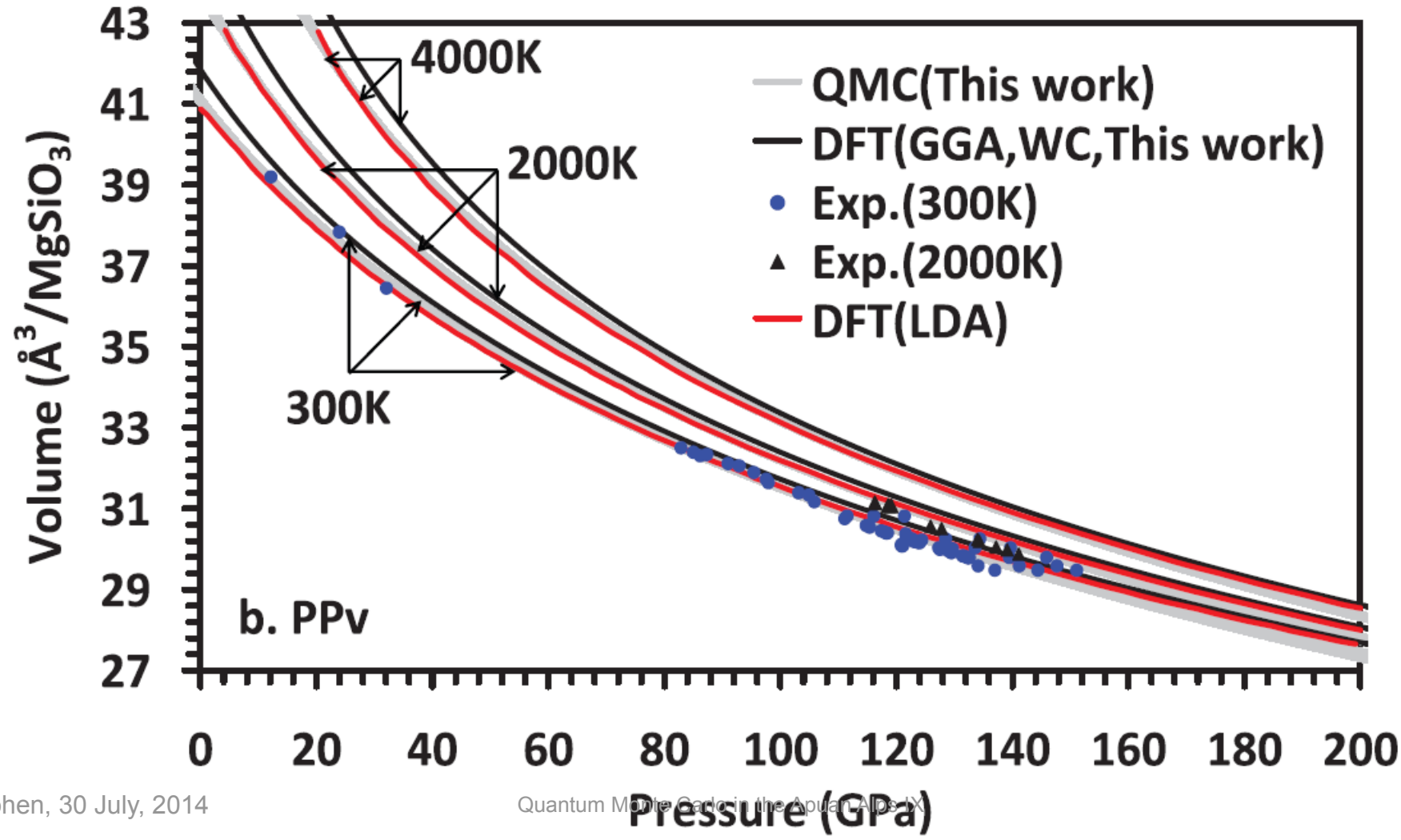

Pv-PPv Volume difference at 300K

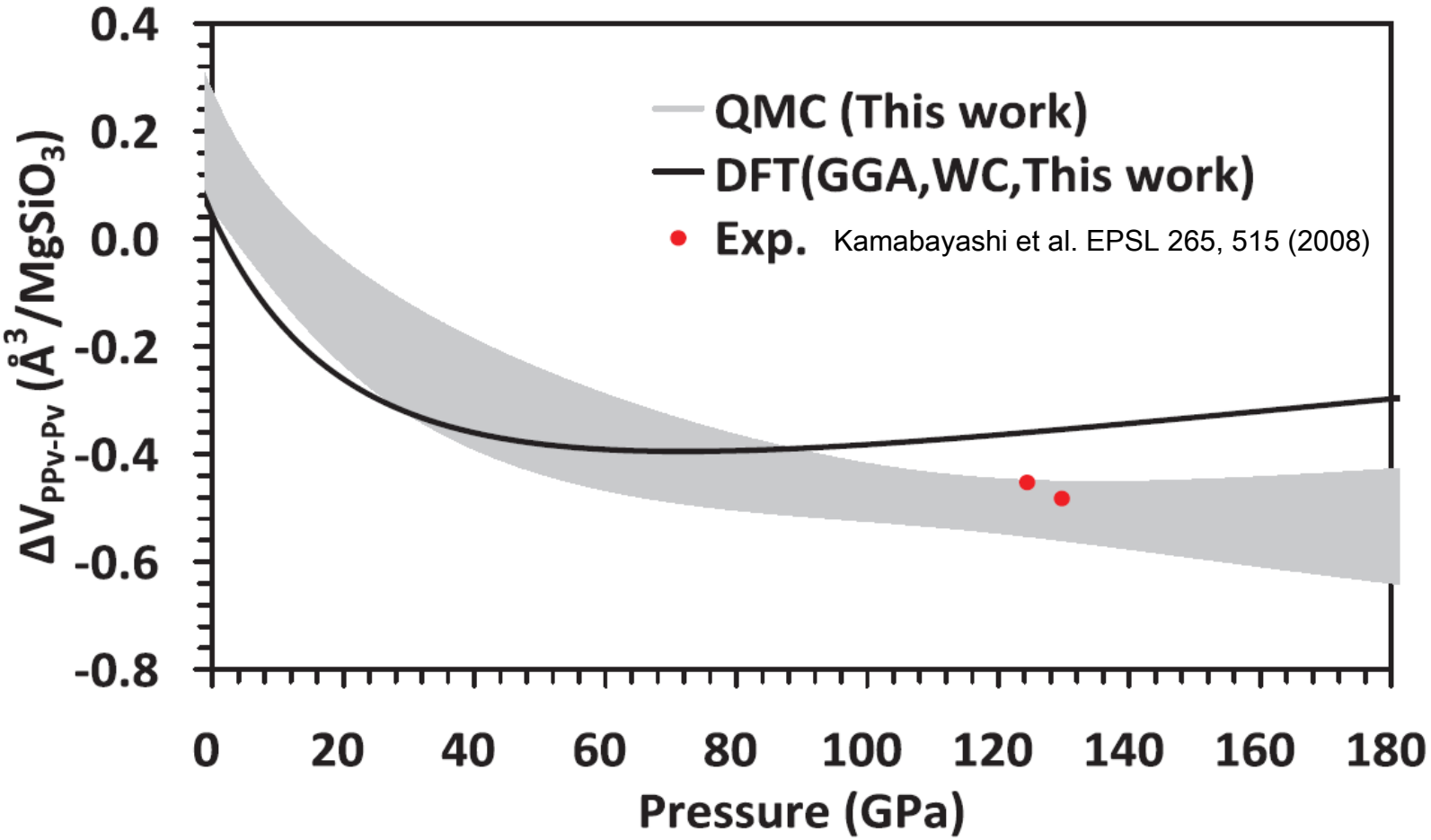

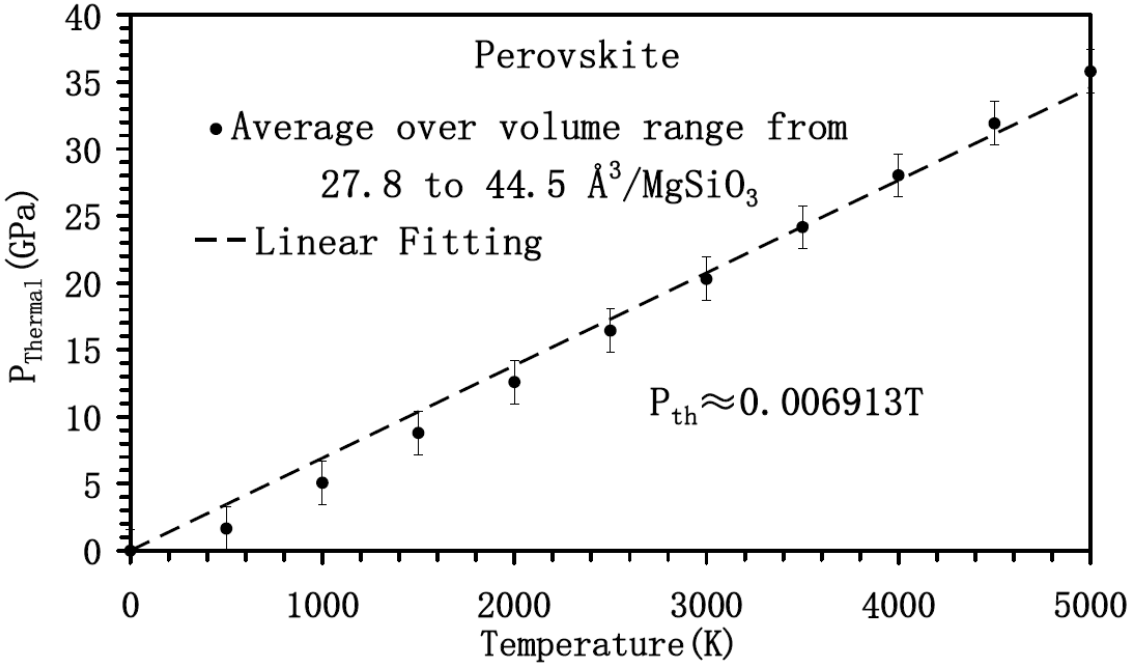

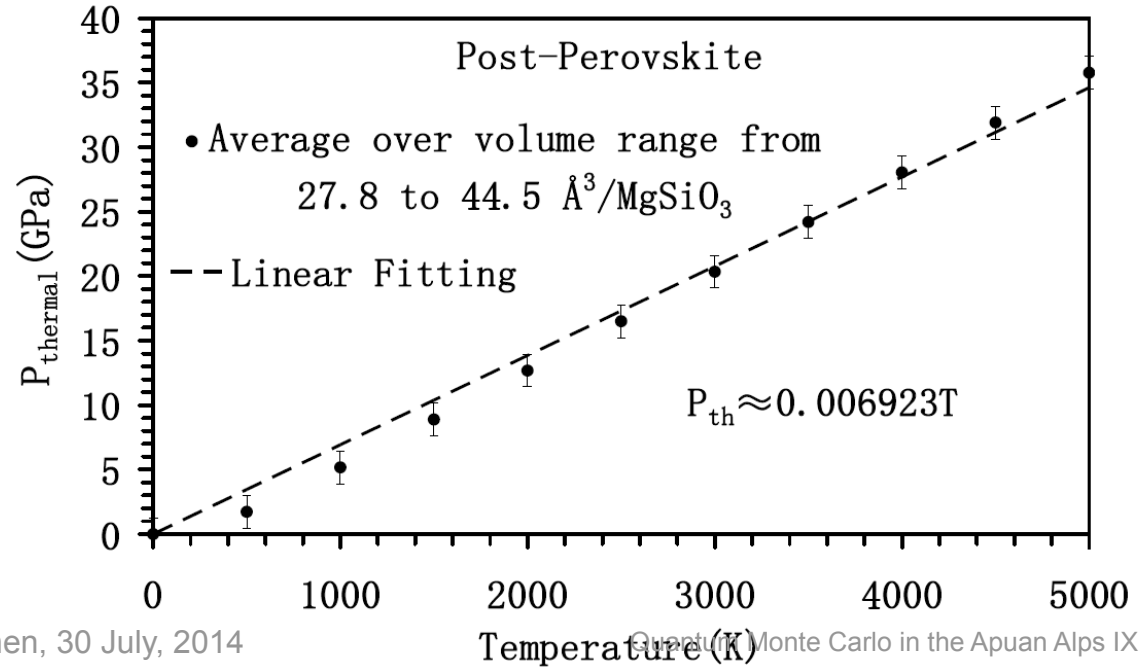

Thermal pressure from quasiharmonic lattice dynamics with DFT

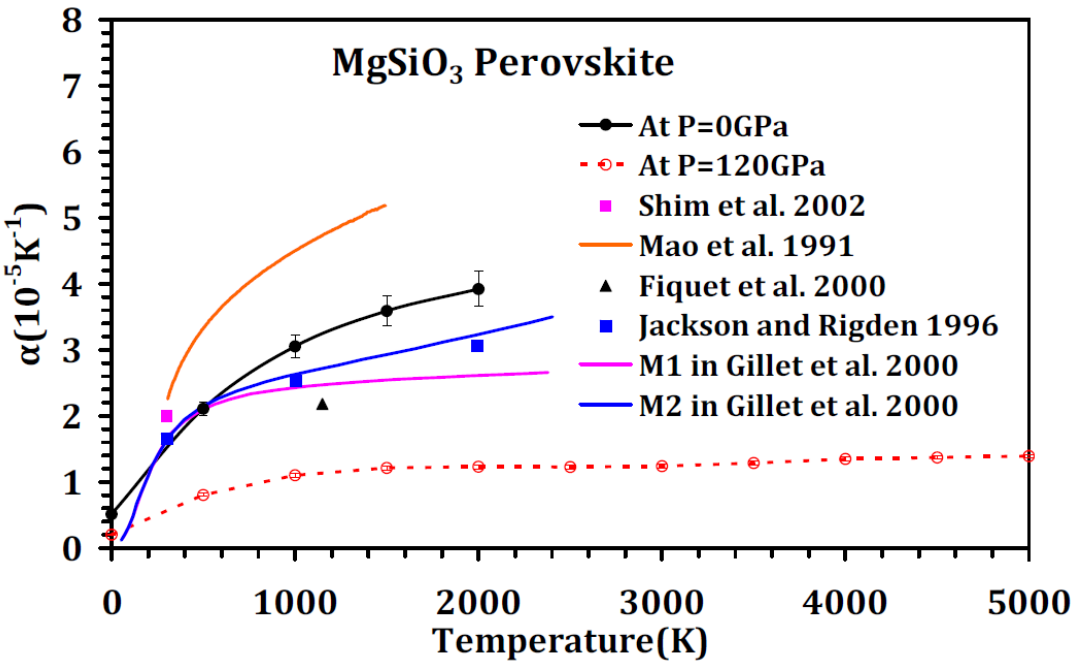

Thermal Expansivity

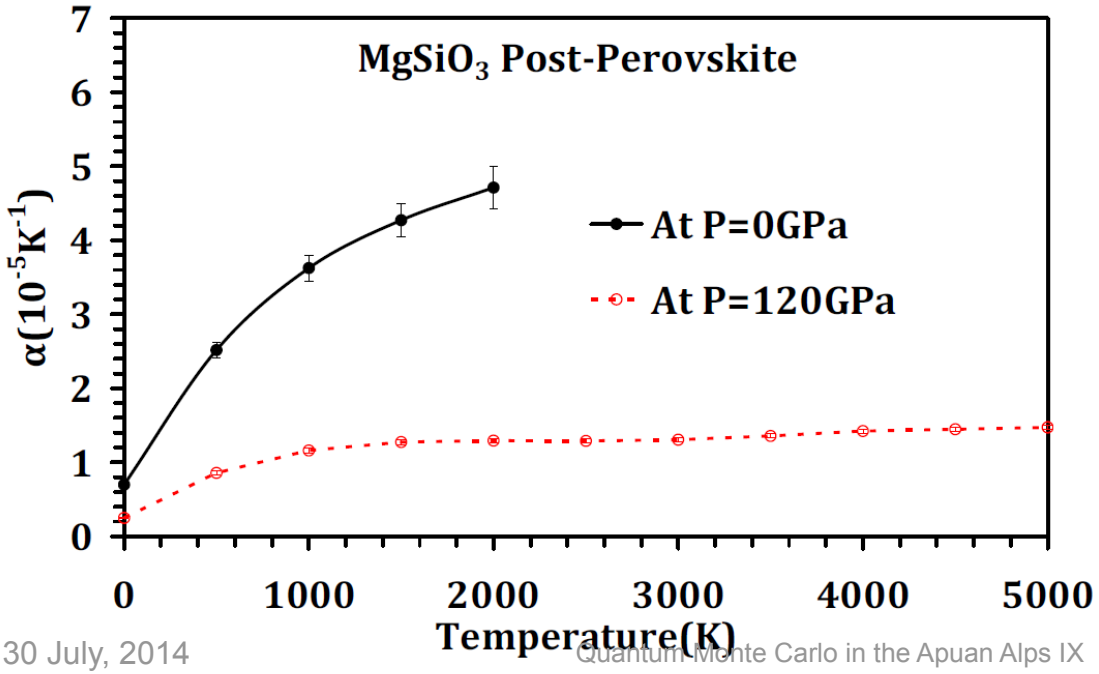

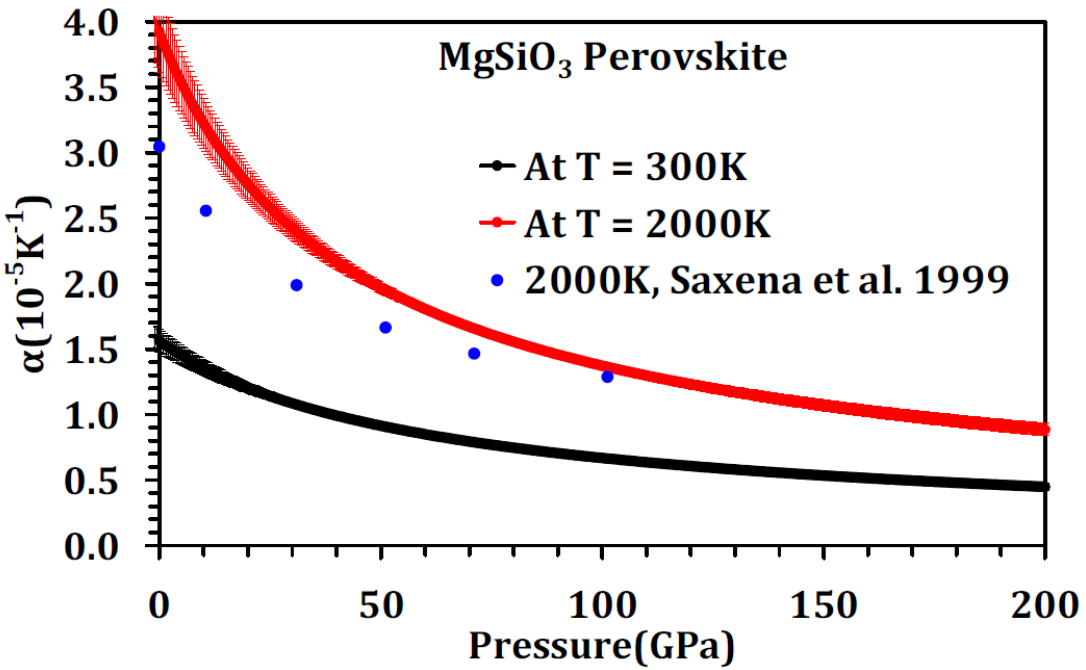

Isotherm for Thermal Expansivity

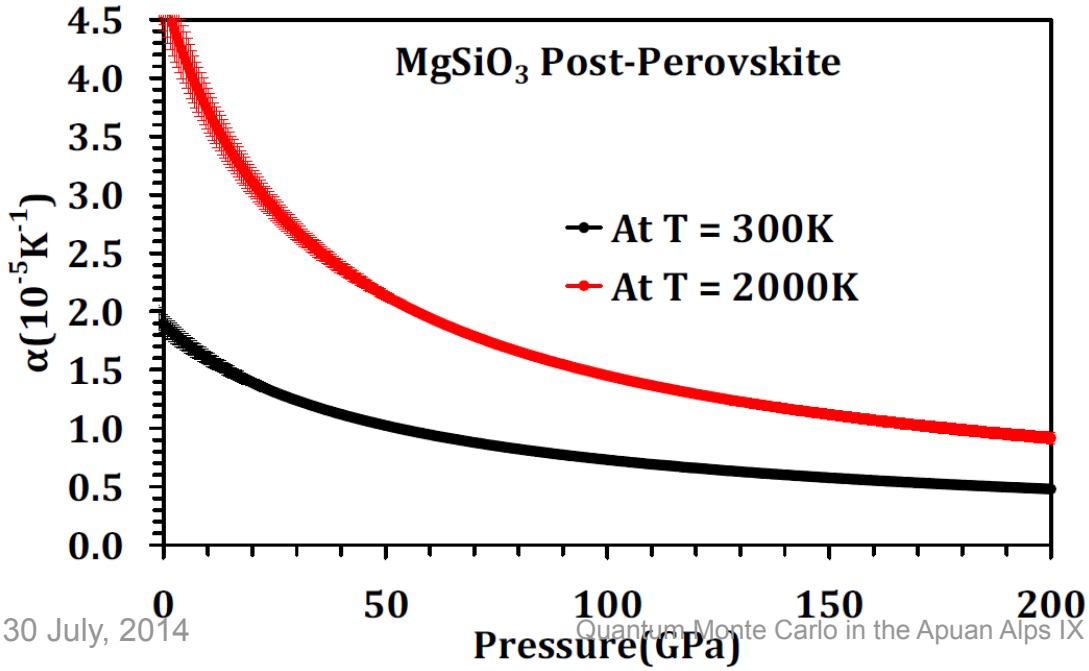

MgSiO3 Perovskite and Post-Perovskite Phases Transition Pressure

Phases transition occurs at ΔG = 0

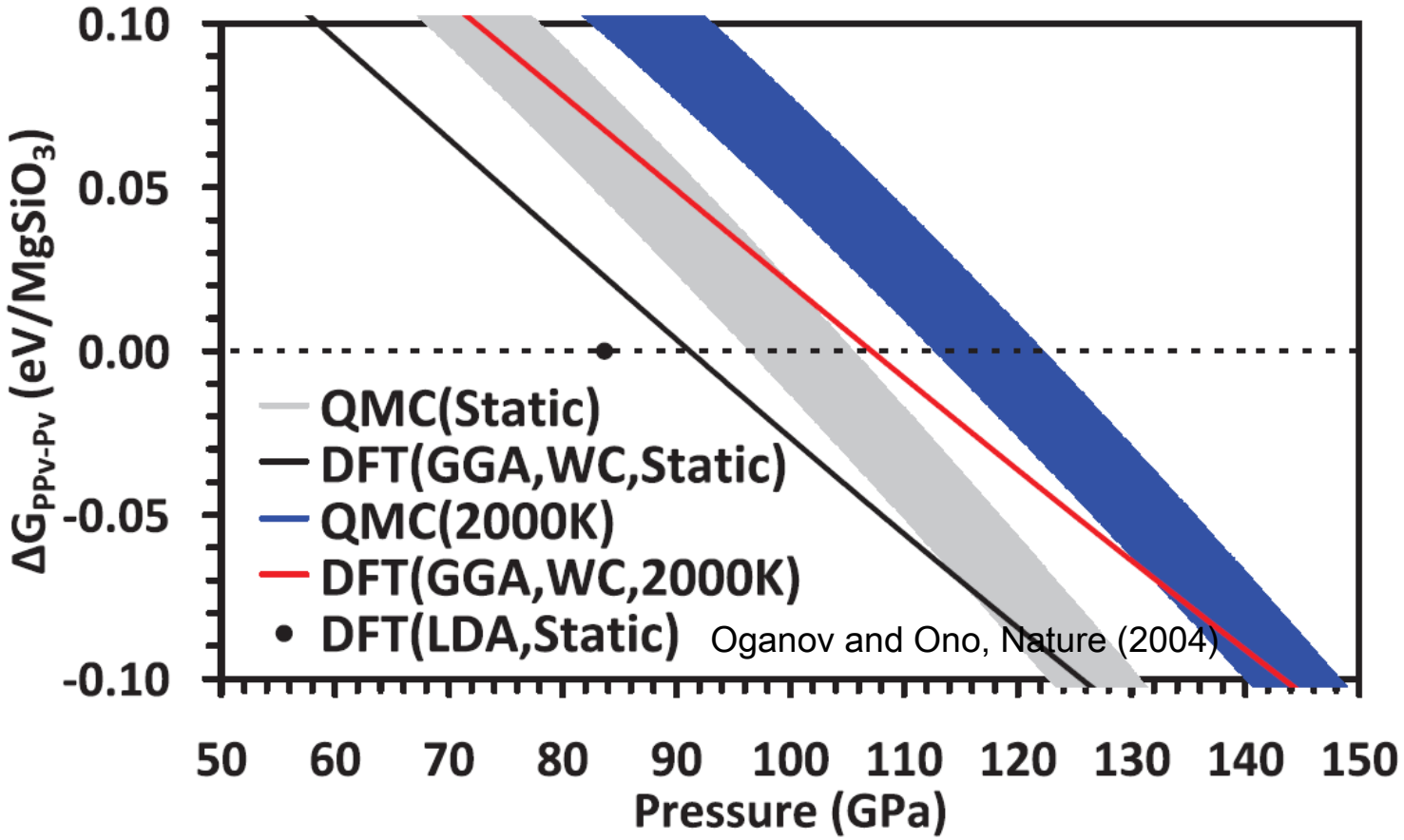

$MgSiO_3$ Perovskite and Post-Perovskite Phase Boundary

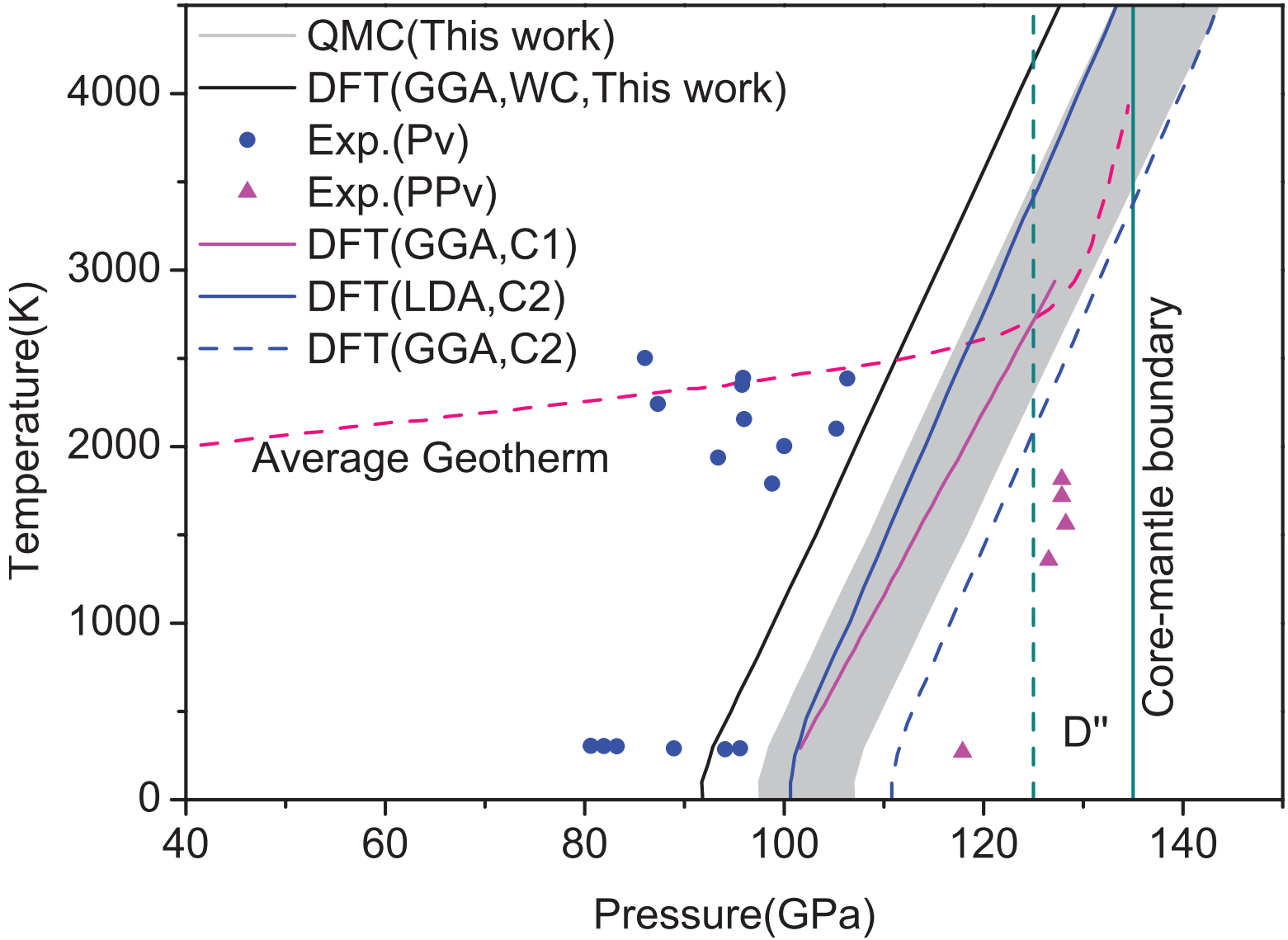

Post-perovskite
The Last Mantle Phase Transition?

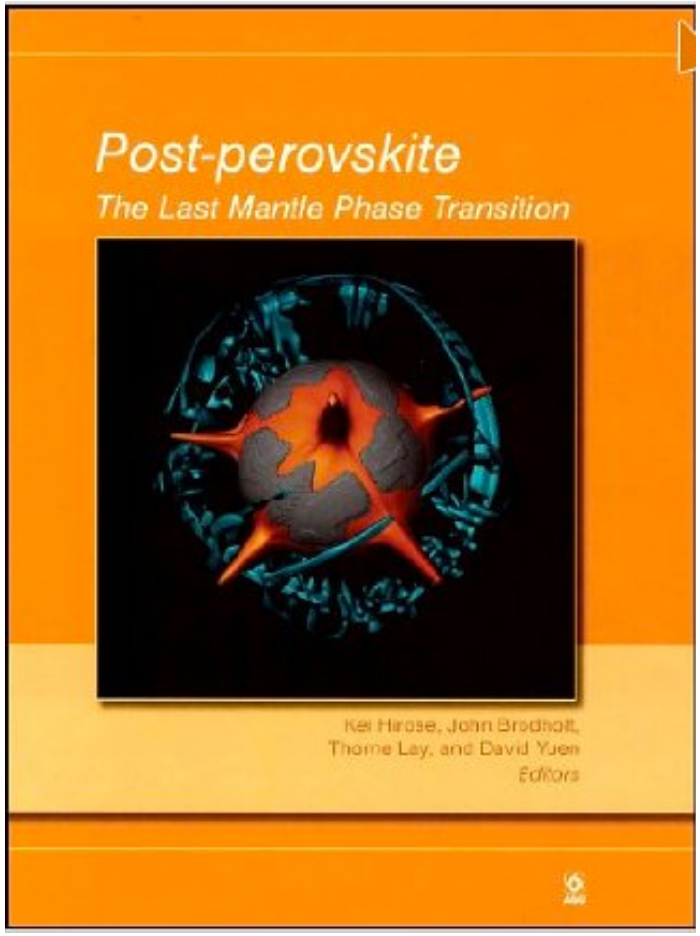

DEEP EARTH

Disproportionation of $(Mg,Fe)SiO_3$ perovskite in Earth's deep lower mantle

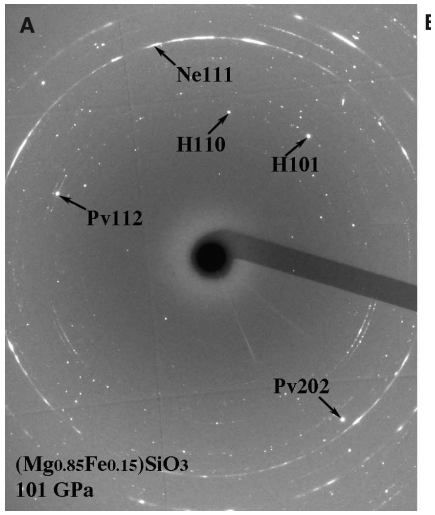

Li Zhang,[1,2]* Yue Meng,[3] Wenge Yang,[1,4] Lin Wang,[1,4] Wendy L. Mao,[5,6] Qiao-Shi Zeng,[5] Jong Seok Jeong,[7] Andrew J. Wagner,[7] K. Andre Mkhoyan,[7] Wenjun Liu,[8] Ruqing Xu,[8] Ho-kwang Mao[1,2]

The mineralogical constitution of the Earth's mantle dictates the geophysical and geochemical properties of this region. Previous models of a perovskite-dominant lower mantle have been built on the assumption that the entire lower mantle down to the top of the D″ layer contains ferromagnesian silicate [$(Mg,Fe)SiO_3$] with nominally 10 mole percent Fe. On the basis of experiments in laser-heated diamond anvil cells, at pressures of 95 to 101 gigapascals and temperatures of 2200 to 2400 kelvin, we found that such perovskite is unstable; it loses its Fe and disproportionates to a nearly Fe-free $MgSiO_3$ perovskite phase and an Fe-rich phase with a hexagonal structure. This observation has implications for enigmatic seismic features beyond ~2000 kilometers depth and suggests that the lower mantle may contain previously unidentified major phases.

Higgs Physics Suggests The Universe Shouldn't Exist

YIKES: Here's What Would Happen If The Earth Suddenly Stopped Spinning

Prehistoric Poop Yields Big Surprise About Neanderthals

Weird Rocks Support New Model For Earth's Deep Mantle

LiveScience | By Becky Oskin

Posted: 05/23/2014 8:51 am EDT | Updated: 05/23/2014 8:59 am EDT

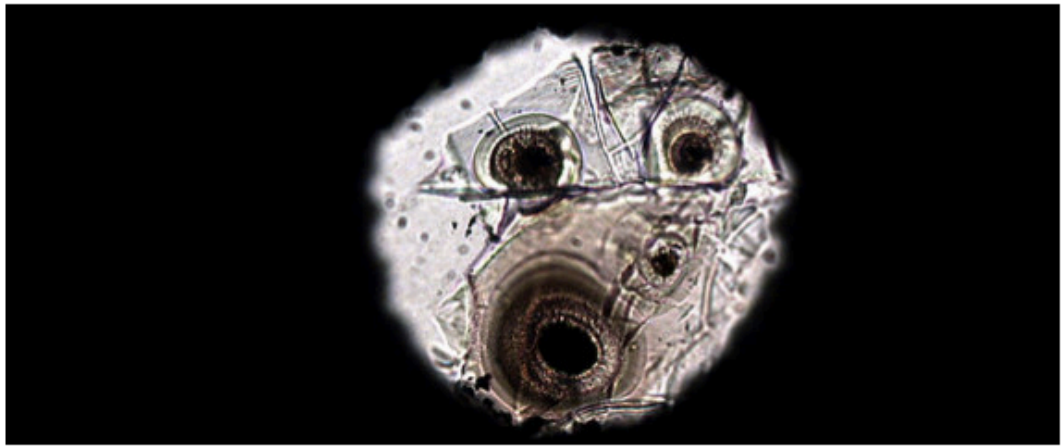

630 Like | 217 Share | 42 Tweet | 11 Share | 16 Email

Models of how the Earth's mantle works may need to change, thanks to two new studies that recreate the extreme conditions just above the planet's core.

H-phase, a New Phase of Silicate in the Earth's Mantle?

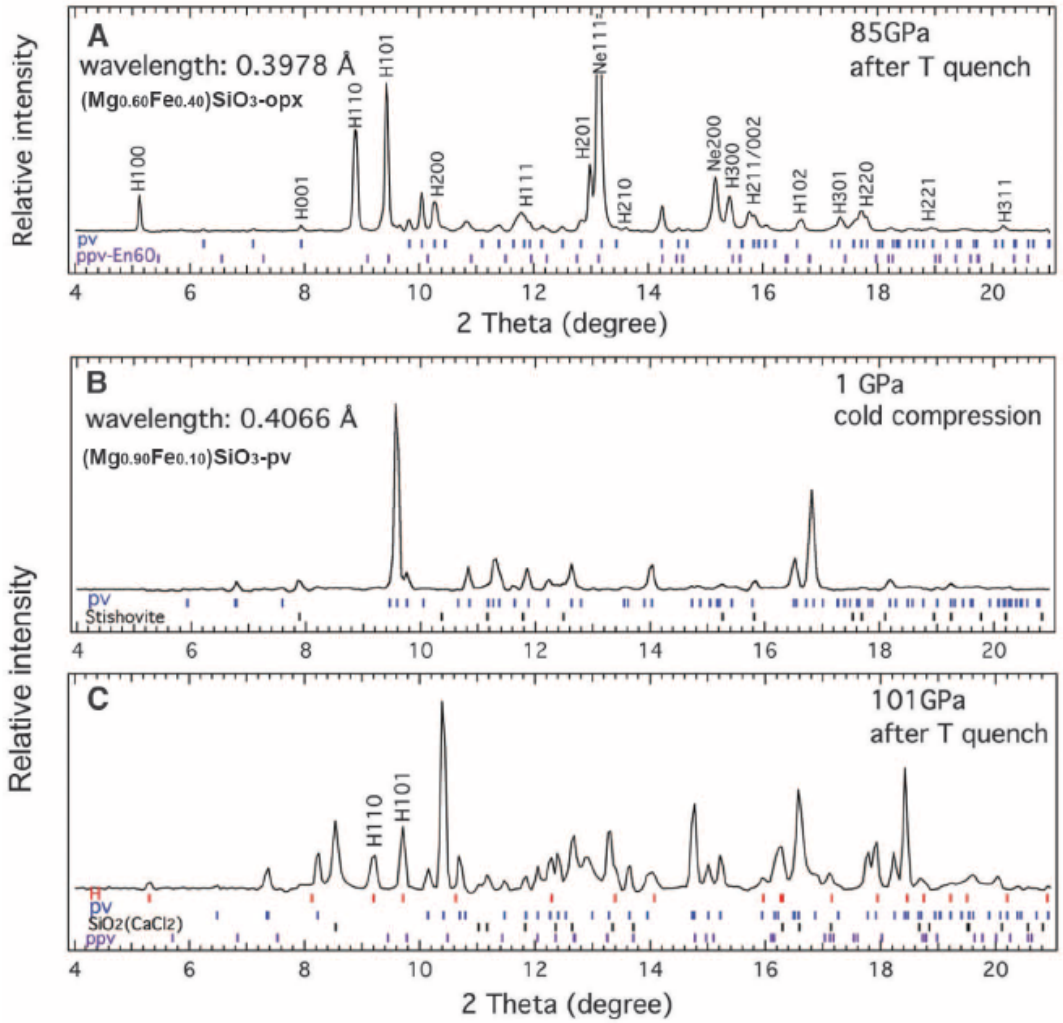

Zhang et al., Science 2014, claim discovery of a new phase of (Mg,Fe)SiO3 they call the H phase based on X-ray powder diffraction.

They say the H-phase has hexagonal structure.

Atomic positions in the unit cell of H-phase are unknown.

L. Zhang, et al. Science **344**, 877 (2014)

Structure Evolution Algorithm in XtalOpt

1. Random Sampling

Given component atoms and ranges of lattice parameters

2. Genetic Algorithms

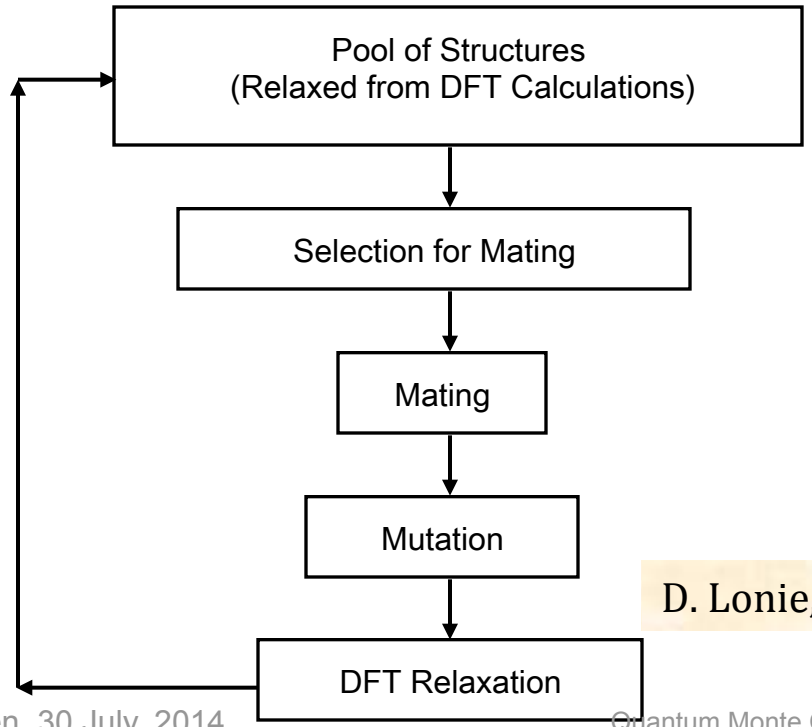

$$p_i = C\left(1 - \frac{H_i - H_{\min}}{H_{\max} - H_{\min}}\right) \qquad \sum_i p_i = 1$$

*p*i, selection probability of structure *i*

*H*i, DFT enthalpy of structure *i*

C normalization constant

D. Lonie, and E. Zurek, Comp. Phys. Comm. **182**, 372 (2011)

Mating and Mutation Operators

Crossover, Strain, Exchange, Ripple, and their hybrids

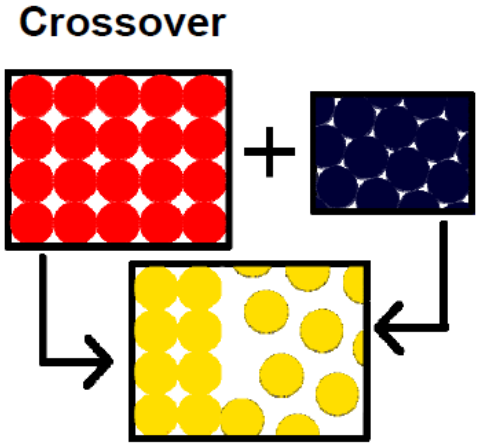

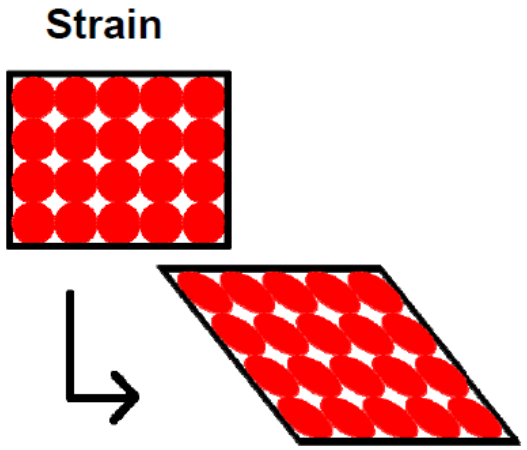

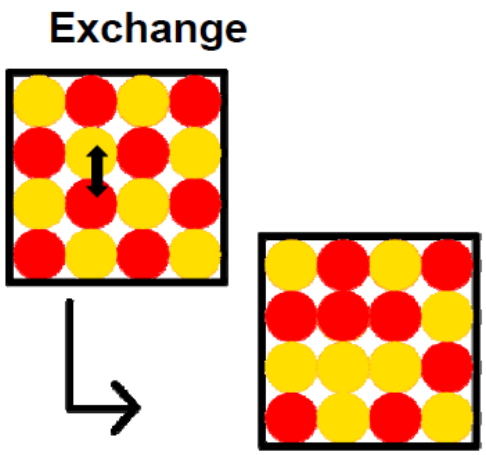

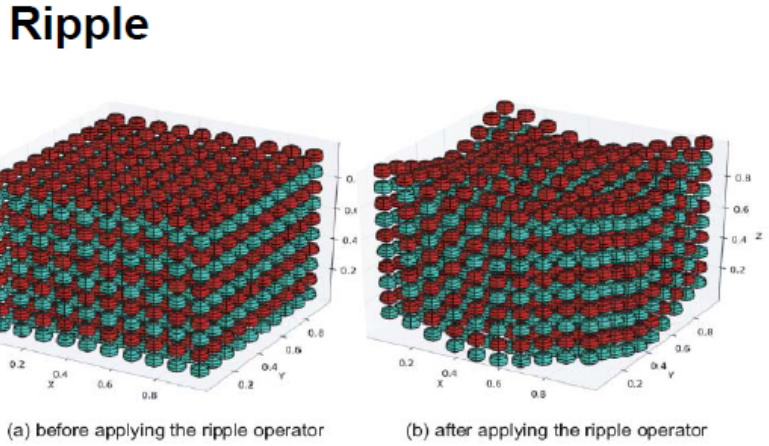

D. Lonie, and E. Zurek, Comp. Phys. Comm. **182**, 372 (2011)

PPv-II Structure, Comparison with PPv

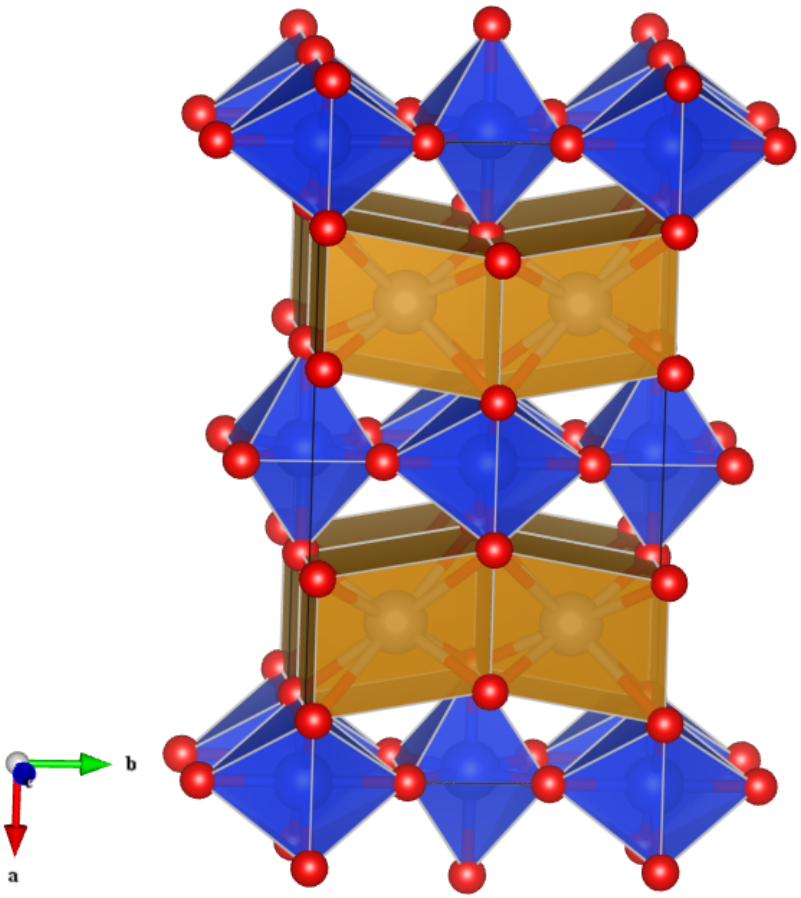

PPv-II, ChM

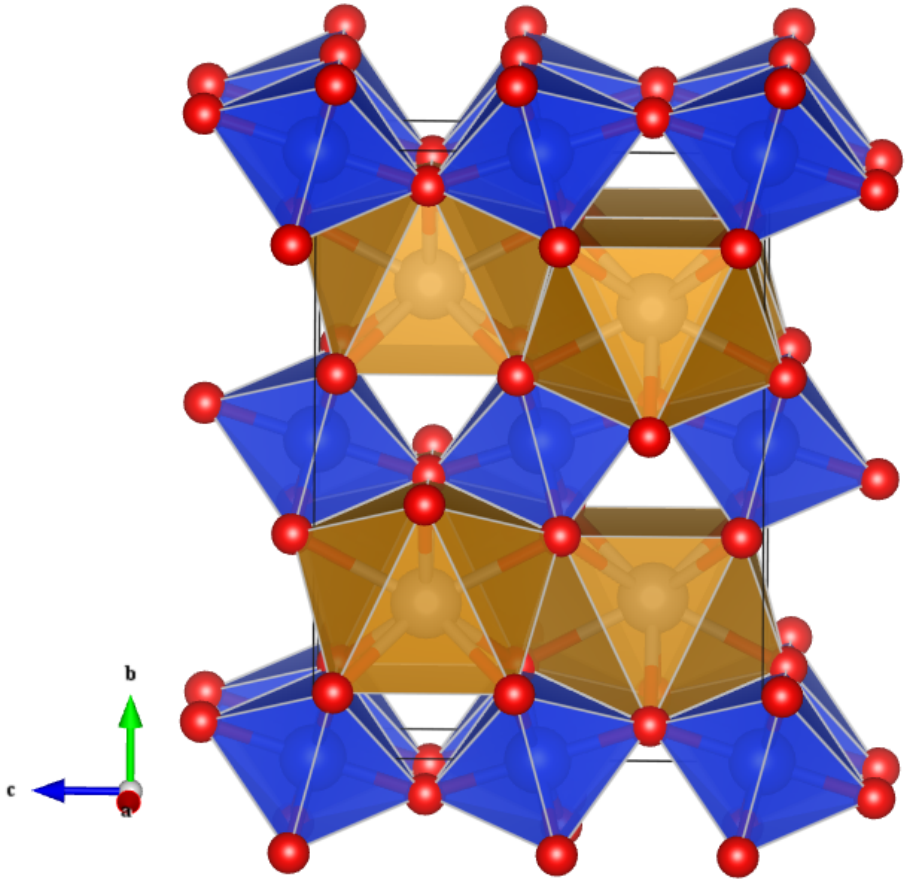

PPv, Cecum

X-ray Diffraction Pattern, Comparison II

"The XRD peaks are almost for pure H-phase"

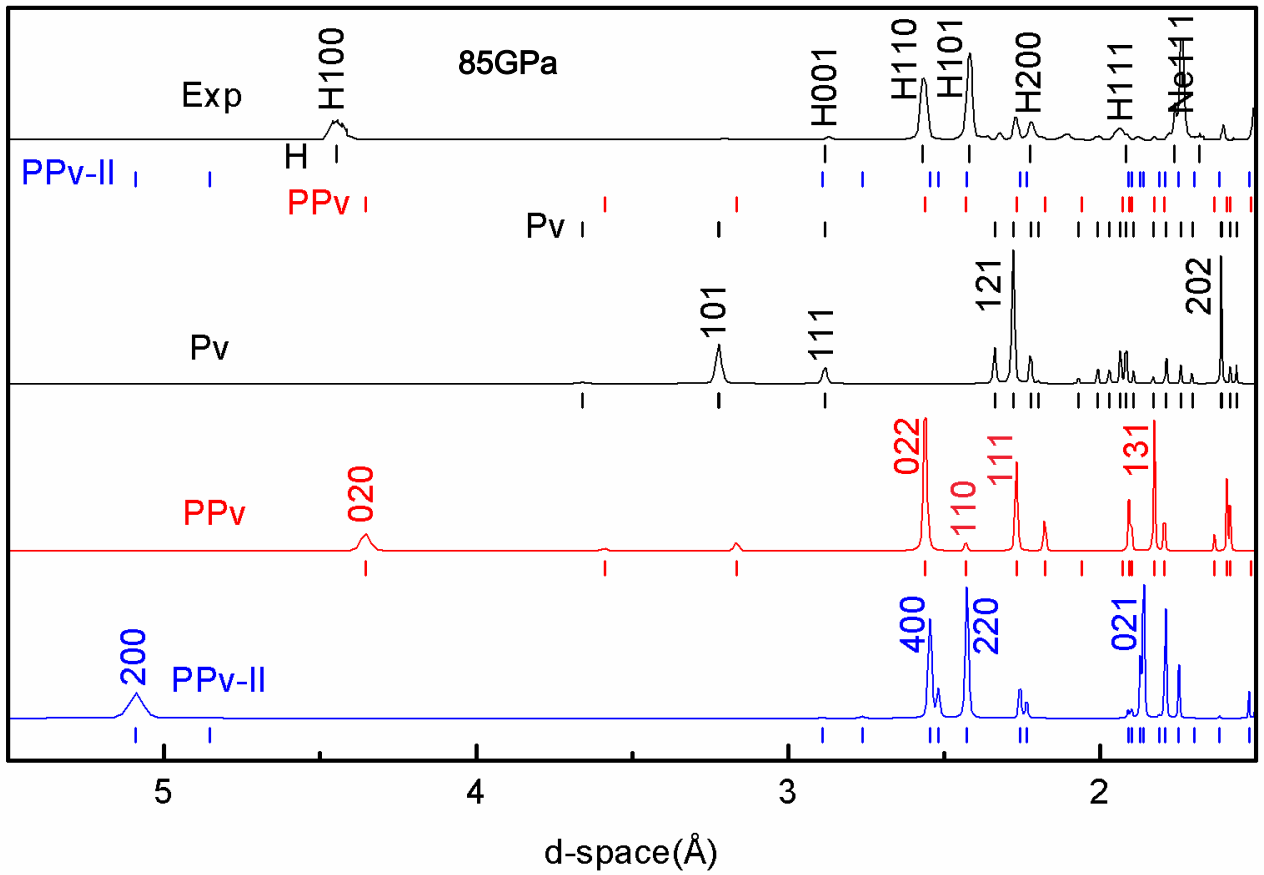

Pv: MgSiO3

PPv: FeSiO3

PPv-II: FeSiO3

*Two main peaks of H-phase compare well with those of PPv-II FeSiO3. PPv-II has more peaks.

Phase Stability of Pv, PPv and PPv-II phases

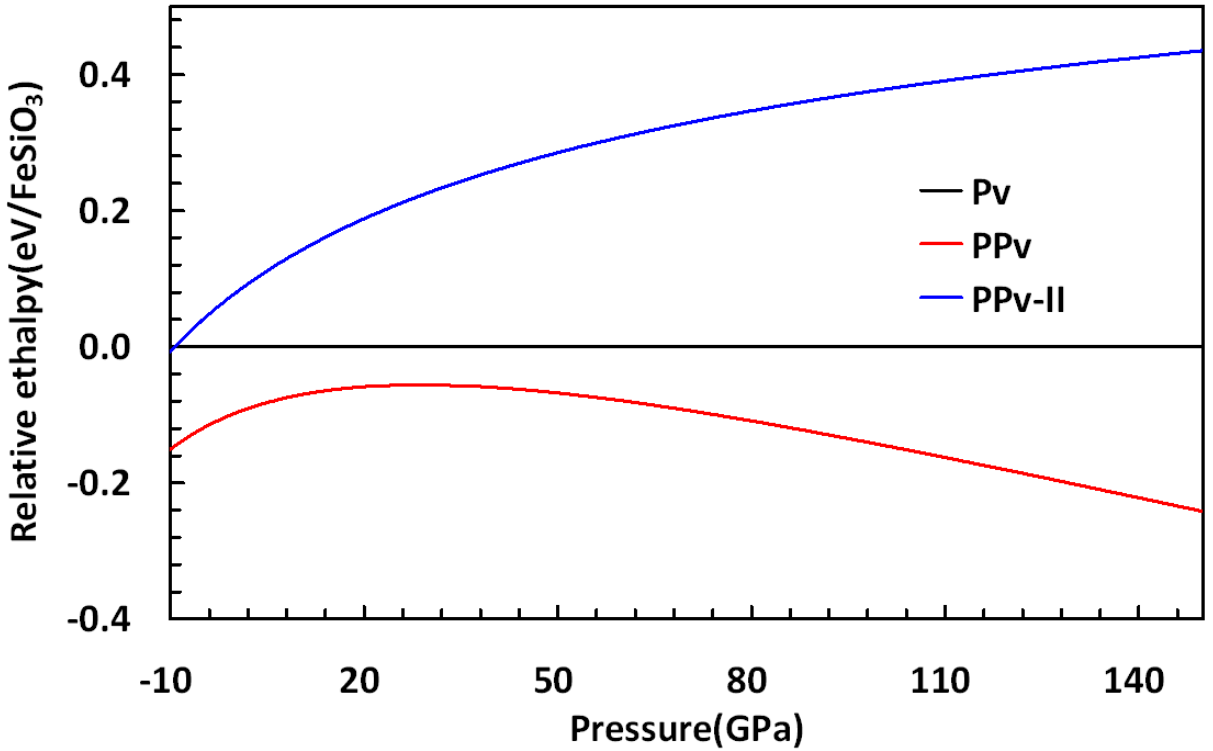

Both Pv and PPv phases of $FeSiO_3$ are more stable than PPv-II at T=0 K.

It is possible that PPv-II became stable at high temperature.

PPv-II continuous phase transition at lower pressures

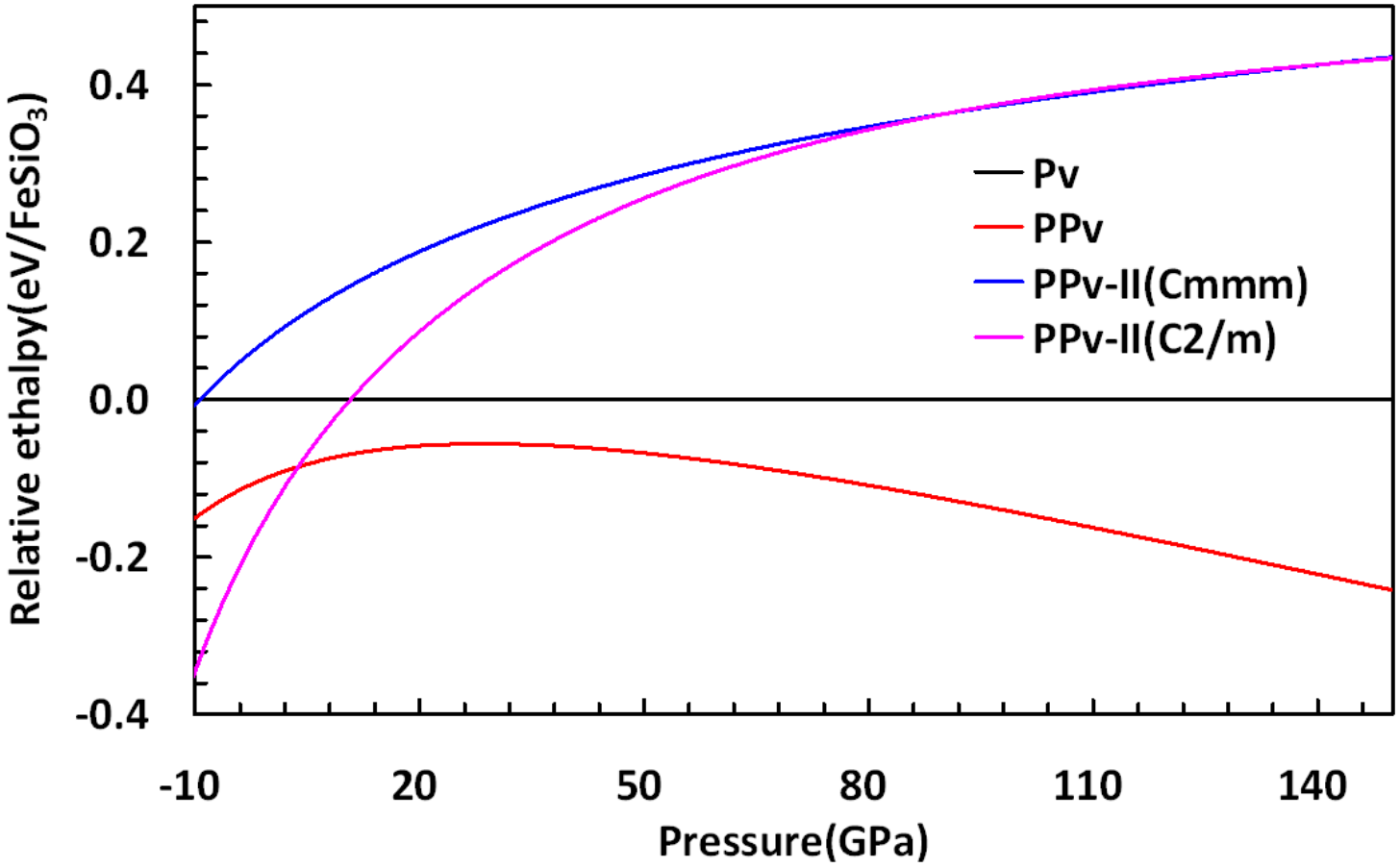

At low pressures, Cmmm goes to C2/m via small displacements.

Background: FeO

- At ambient pressure FeO is an antiferromagnetic insulator with a rock salt structure
- Iron 3d states partially filled, but localized
- Borderline between charge transfer and Mott insulator
- Difficult to make stoichiometric FeO in the lab at low pressures (vacancies yield $Fe_{1-x}O$ where x ~ 0.07) but stoichiometric under pressure

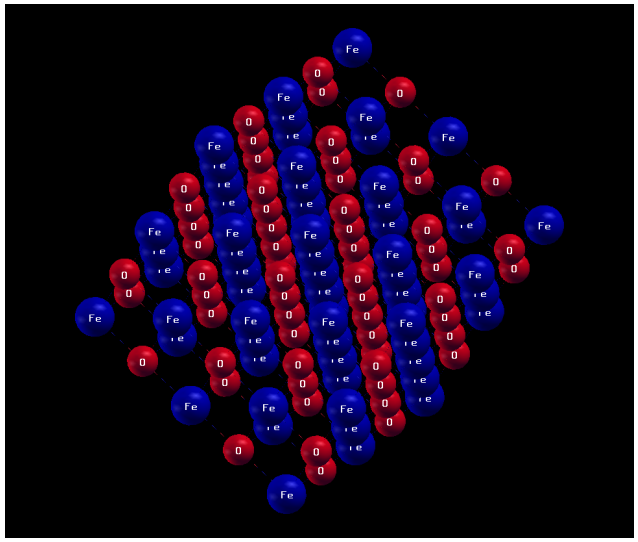

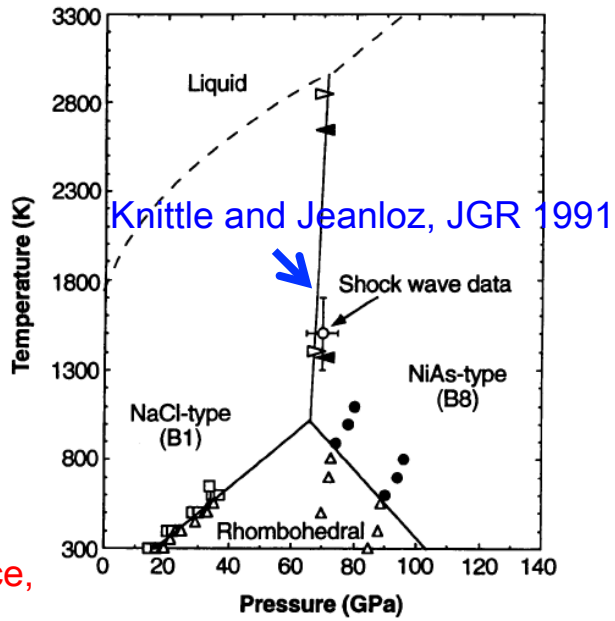

The phase diagram as of 1994 (Fei and Mao, Science, 266, 1678, 1994)

FeO wüstite is an insulator at ambient conditions

- LDA/GGA etc. make it a metal

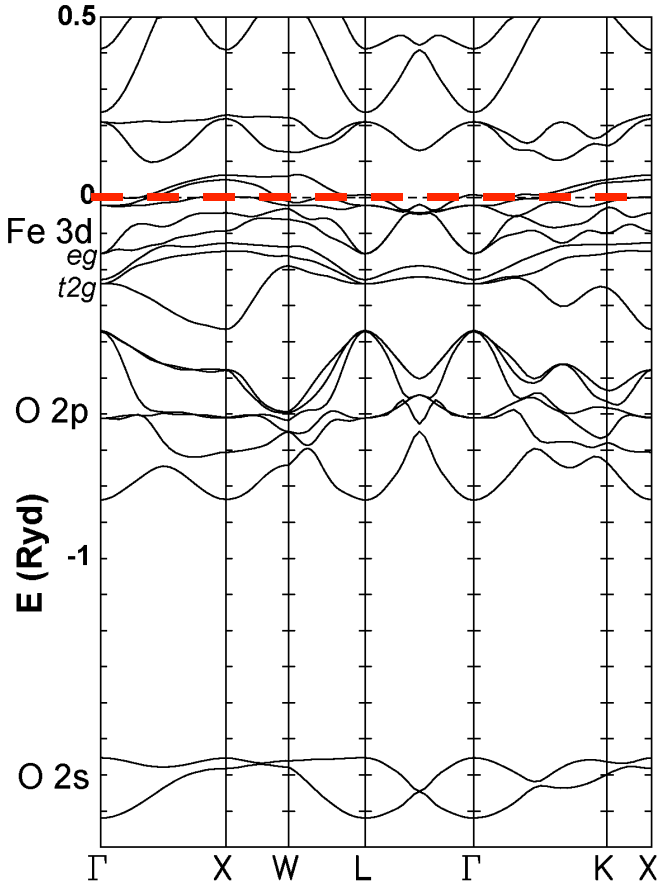

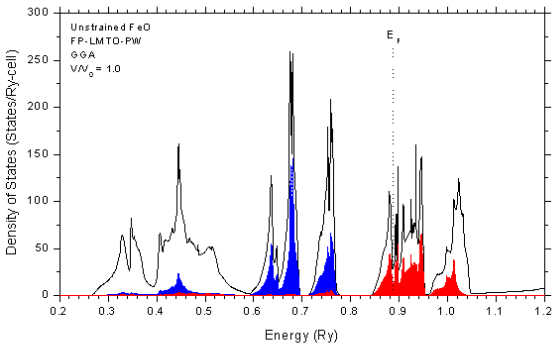

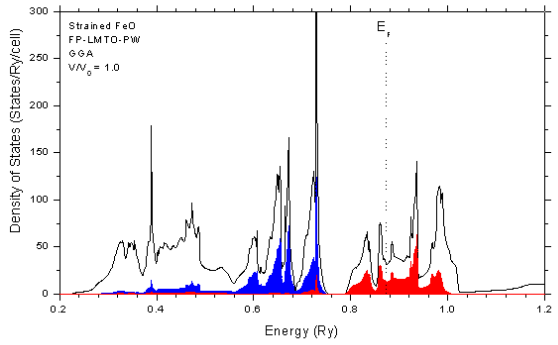

- LDA+U does open a gap in AFM rhombohedral or lower symmetry FeO and predicts a metal insulator transition under pressure, but not a high-spin low-spin transition. (Gramsch, Cohen, and Savrasov, Am. Mineral., **88**, 257 (2003).
- LDA+U is a model, and how accurate it is unknown.
- LDA+U cannot give a gap in paramagnetic FeO.

Cohen et al. (1998) High-Pressure Materials Research. Materials Research Society. **499**.

Magnetic Collapse in Transition Metal Oxides at High Pressure: Implications for the Earth

Ronald E. Cohen,* I. I. Mazin, Donald G. Isaak

654 SCIENCE • VOL. 275 • 31 JANUARY 1997

Extended Stoner model

Increase in bandwidth causes spin collapse:

$$I\tilde{N}(M) = 1$$

$$\tilde{N}(M) = \frac{M}{\Delta\varepsilon_x}$$

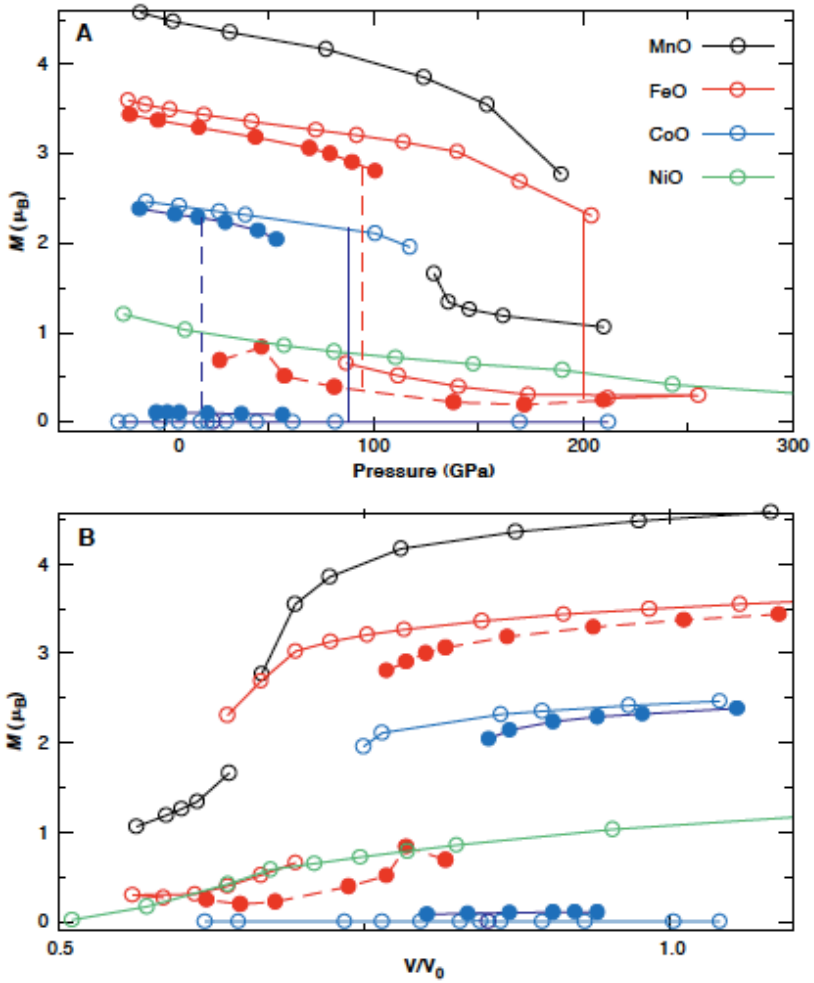

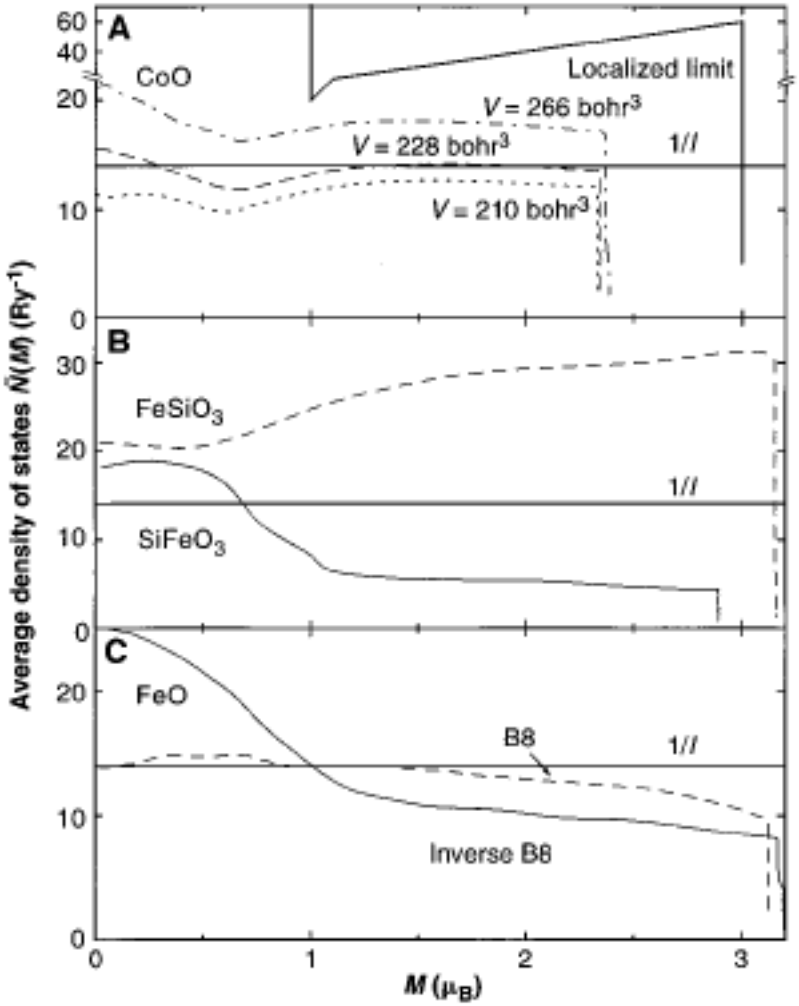

Magnetic collapse vs. High-spin low-spin transition vs. Orbital ordering in FeO

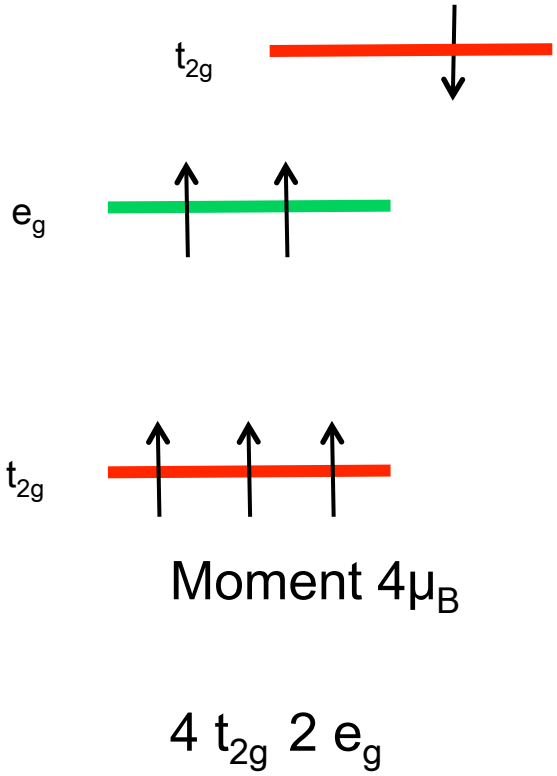

Moment $4\mu_B$

$4\ t_{2g}\ 2\ e_g$

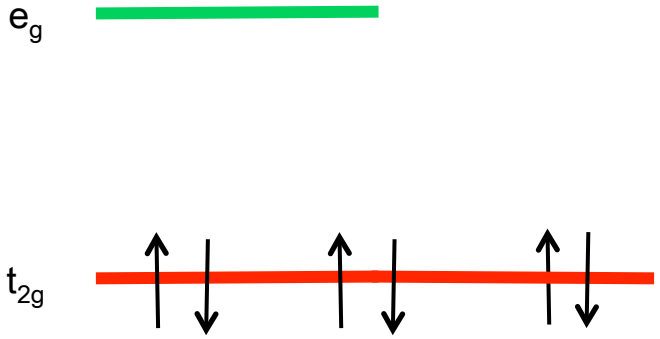

Moment 0

$6\ t_{2g}$

Note: LDA+U cannot give an insualting state for cubic FeO

LDA-DMFT

$H = \sum h + \sum t_{ij} c_{i\alpha}^{\dagger} c_{j\beta}$ Lattice Problem (contains geometry)

$$\Phi[\rho, G_{loc}] = E_H[\rho] + E_{xc}^{LDA}[\rho] + \tilde{\Phi}[G_{loc}] - \Phi_{DC}[n]$$

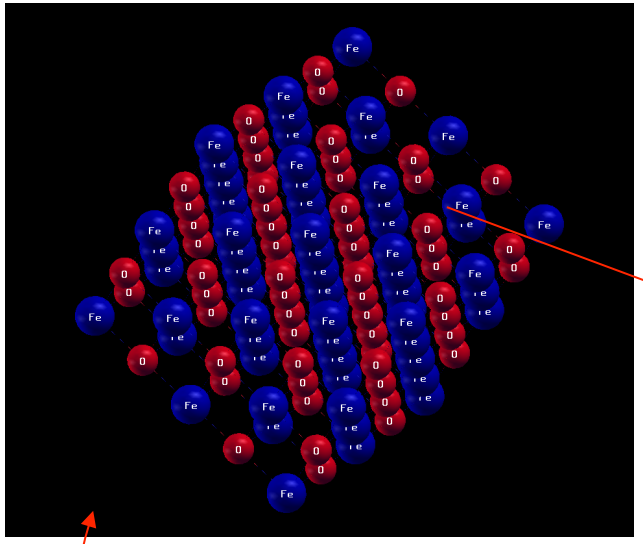

Fully self-consistent, finite temperature

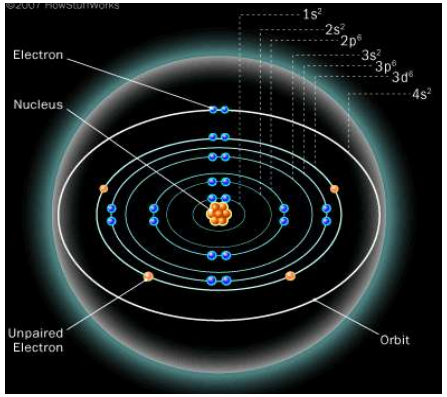

Lattice Problem (DFT) LAPW

Atomic Problem
(Many-body theory: DMFT)

$$S_{imp} = S_{atom} + \int\int dt\, dt'\, c_{\alpha}^{\dagger} \nabla(t - t') c_{\beta}$$

New density

∇ → Impurity Model (CTQMC) → G_{imp}

H_{DFT} → Impurity Model (CTQMC) → Σ

DFT-DMFT

$$G(\vec{k},i\omega)=[(i\omega+\mu)O(\vec{k})-H^{KS}(\vec{k})-\Sigma'(i\omega)]^{-1}$$

Crystal problem

$$G_{imp}=\frac{1}{\omega-E_{imp}-\Sigma-\Delta}=G_{loc}=\sum_{\mathbf{k}}\frac{1}{G_0^{-1}(\mathbf{k})-\Sigma}.$$

"Impurity" problem

$$P\left(\omega+\mu-H^{KS}-\mathrm{E}\Sigma'\right)^{-1}=\left(\omega-E_{imp}-\Sigma_{imp}-\Delta\right)^{-1}$$

Self-consistency condition

Kristjan Haule DFT-DMFT code:

integrates wien2k LAPW code for Crystal with Continuous Time Quantum Monte Carlo (CTQMC) for impurity

Fully self-consistent in charge density ρ, chemical potential μ, impurity levels E_{imp}, hybridization Δ, and self-energy Σ.

No down folding, fully self-consistent

Calculations are done on imaginary frequency ω axis, and analytically continued to real axis.

Both Hubbard interaction and Hund's coupling are included in CTQMC

$$
\begin{aligned}
H_I &= \sum_{L_a,\cdots,L_d,m,\sigma\sigma'} \sum_{k=0}^{2l} \frac{4\pi F^k_{\{l\}}}{2k+1} \langle Y_{L_a} | Y_{km} | Y_{L_c} \rangle \\
&\times \langle Y_{L_d} | Y^*_{km} | Y_{L_b} \rangle f^\dagger_{L_a,\sigma} f^\dagger_{L_b,\sigma'} f_{L_d,\sigma'} f_{L_c\sigma}
\end{aligned}
$$

Y_L are spherical harmonics

$F^k_{\{l\}}$ are Slater integrals

F^0 is the Hubbard U, derived from cRPA, cLDA or GW

$F^2, \cdots, F^6$ are reduced by 30% of their atomic values due to screening effects

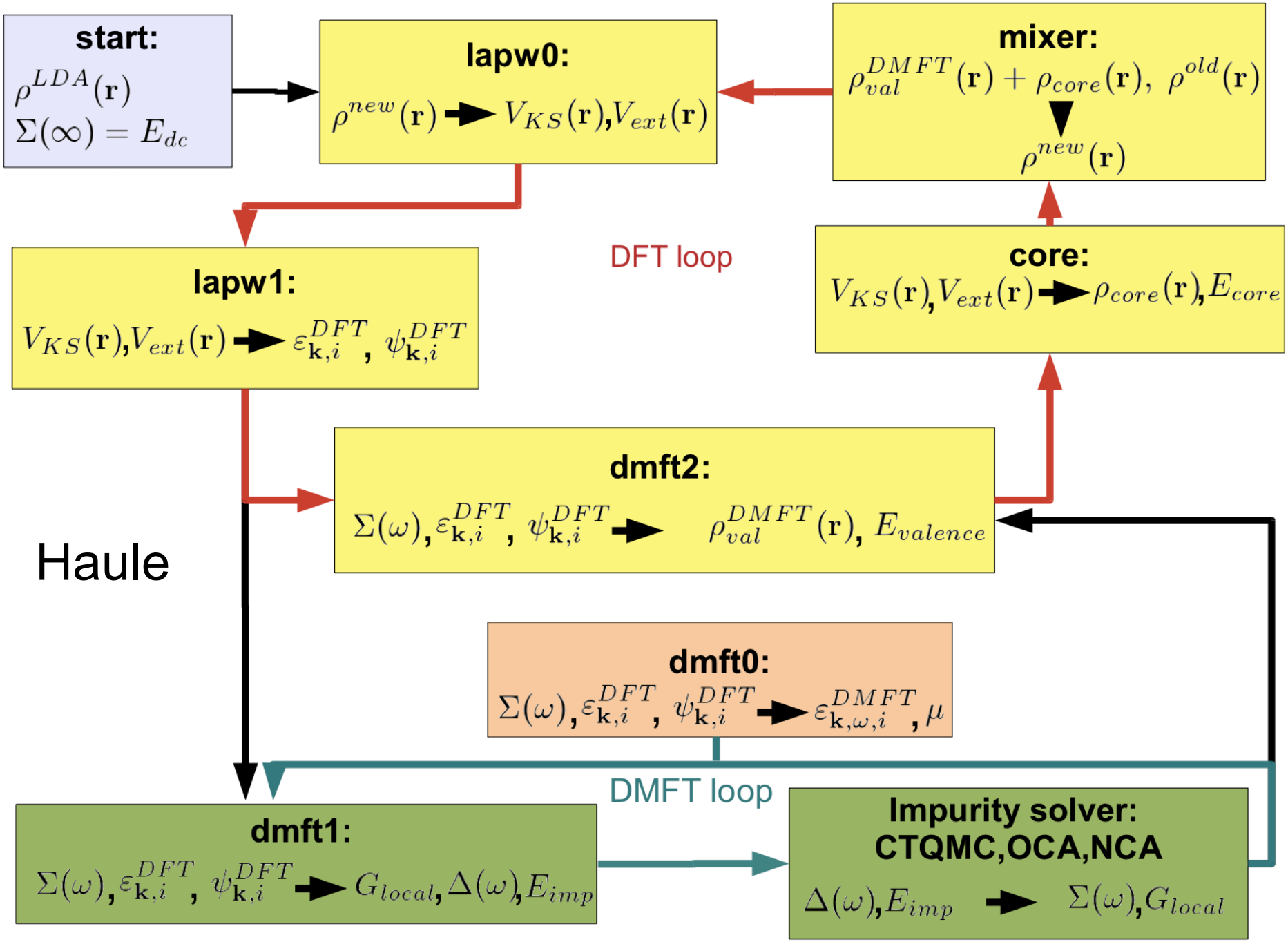
start:
$\rho^{LDA}(\mathbf{r})$
$\Sigma(\infty) = E_{dc}$
lapw0:
$\rho^{new}(\mathbf{r}) \rightarrow V_{KS}(\mathbf{r}), V_{ext}(\mathbf{r})$
mixer:
$\rho_{val}^{DMFT}(\mathbf{r}) + \rho_{core}(\mathbf{r}),\ \rho^{old}(\mathbf{r})$
$\rho^{new}(\mathbf{r})$
DFT loop
lapw1:
$V_{KS}(\mathbf{r}), V_{ext}(\mathbf{r}) \rightarrow \varepsilon_{\mathbf{k},i}^{DFT},\ \psi_{\mathbf{k},i}^{DFT}$
core:
$V_{KS}(\mathbf{r}), V_{ext}(\mathbf{r}) \rightarrow \rho_{core}(\mathbf{r}), E_{core}$
dmft2:
$\Sigma(\omega), \varepsilon_{\mathbf{k},i}^{DFT},\ \psi_{\mathbf{k},i}^{DFT} \rightarrow \rho_{val}^{DMFT}(\mathbf{r}),\ E_{valence}$
Haule
dmft0:
$\Sigma(\omega), \varepsilon_{\mathbf{k},i}^{DFT},\ \psi_{\mathbf{k},i}^{DFT} \rightarrow \varepsilon_{\mathbf{k},\omega,i}^{DMFT}, \mu$
DMFT loop
dmft1:
$\Sigma(\omega), \varepsilon_{\mathbf{k},i}^{DFT},\ \psi_{\mathbf{k},i}^{DFT} \rightarrow G_{local}, \Delta(\omega), E_{imp}$
Impurity solver:
CTQMC,OCA,NCA
$\Delta(\omega), E_{imp} \rightarrow \Sigma(\omega), G_{local}$

Continuous Time Quantum Monte Carlo (CTQMC)

QMC over Feynman diagrams

Imaginary time (frequency)

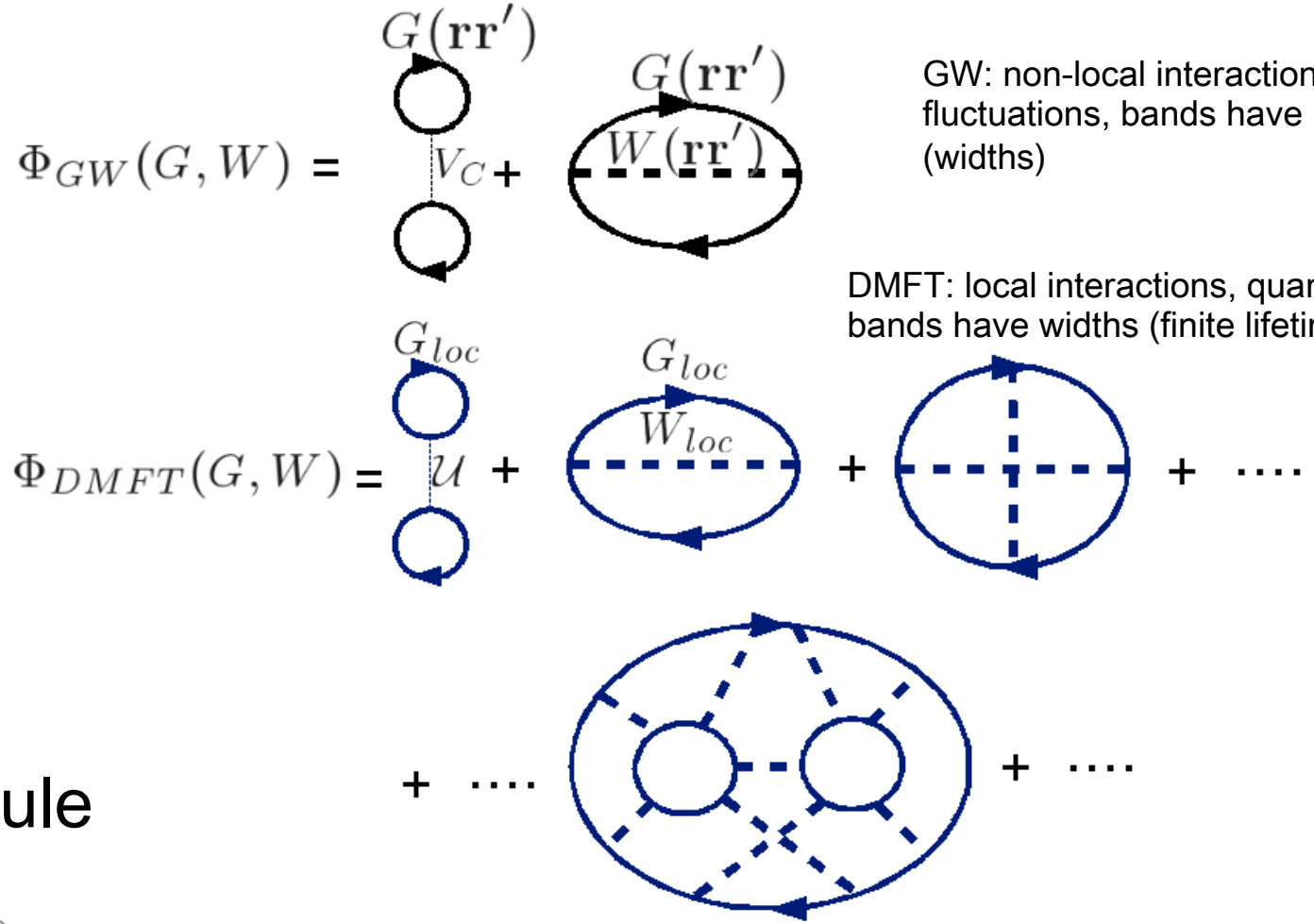

GW: non-local interactions, no quantum fluctuations, bands have infinite lifetimes (widths)

DMFT: local interactions, quantum fluctuations, bands have widths (finite lifetimes)

Haule

CTQMC

$$\Delta S = \sum_{p\sigma,\omega_n} \psi^\dagger_{n\sigma} \frac{V^*_{0p} V_{0p}}{i\omega + \mu - \epsilon_p} \psi_{n\sigma} = \int_0^\beta \int_0^\beta d\tau d\tau' \sum_\sigma \psi^\dagger_\sigma(\tau) \Delta(\tau - \tau') \psi_\sigma(\tau')$$

$$\Delta(i\omega) = \sum_p \frac{V^*_{0p} V_{0p}}{i\omega + \mu - \epsilon_p}$$

$$\begin{aligned} Z &= Z_a \sum_k \frac{1}{k!} \int_0^\beta d\tau_1 \int_0^\beta d\tau'_1 \cdots \int_0^\beta d\tau_k \int_0^\beta d\tau'_k \sum_{\alpha_1 \alpha'_1, \cdots, \alpha_k, \alpha'_k} \\ &\times \langle T_\tau \psi_{\alpha'_1}(\tau'_1) \psi^\dagger_{\alpha_1}(\tau_1) \cdots \psi_{\alpha'_k}(\tau'_k) \psi^\dagger_{\alpha_k}(\tau_k) \rangle_{local} \times \\ &\times \frac{1}{k!} Det \begin{pmatrix} \Delta_{\alpha_1\alpha'_1}(\tau_1, \tau'_1) & \Delta_{\alpha_1\alpha'_2}(\tau_1, \tau'_2) & \cdots & \cdots \\ \cdots & \cdots & \cdots & \cdots \\ \cdots & \cdots & \cdots & \cdots \\ \Delta_{\alpha_k\alpha'_1}(\tau_k, \tau'_1) & \cdots & \cdots & \Delta_{\alpha_k\alpha'_k}(\tau_k, \tau'_k) \end{pmatrix} \end{aligned}$$

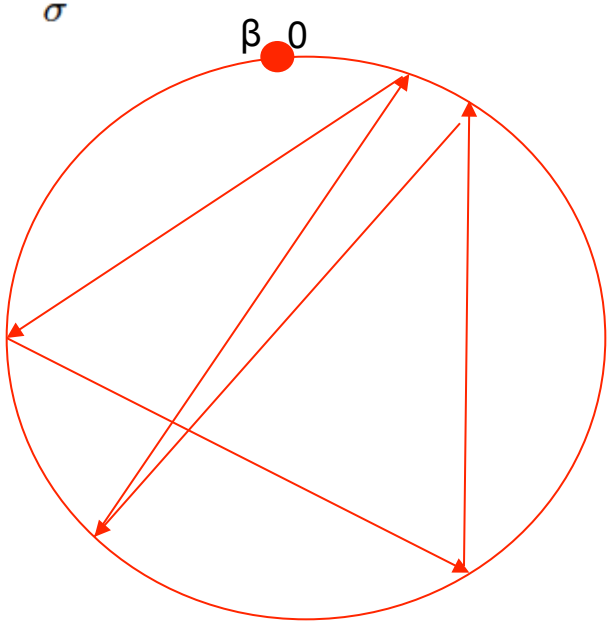

where $Z_a = \int D[\psi^\dagger \psi] e^{-S_a}$ and average is defined by $\langle O \rangle_{local} = \frac{1}{Z} \int D[\psi^\dagger \psi] e^{-S_a} O$.

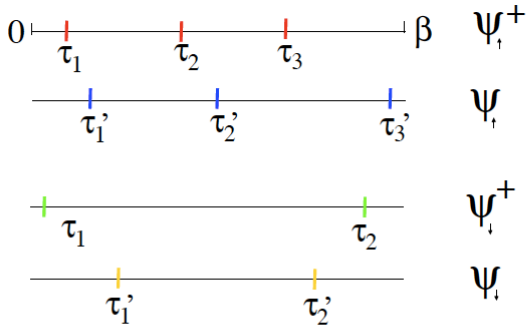

Histogram of number of kinks on Feynman diagrams

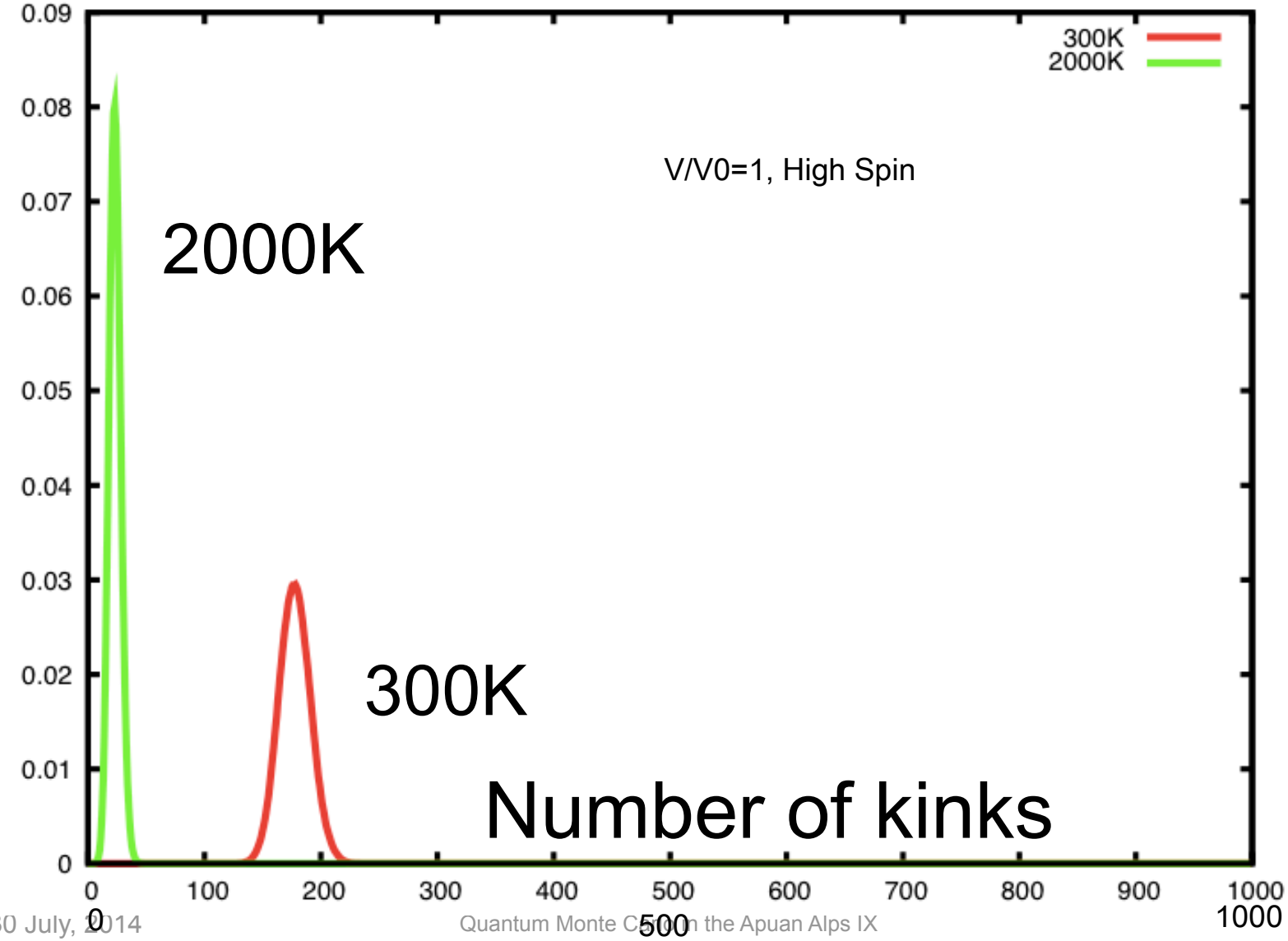

Experimental evidence of metallization at high P and T

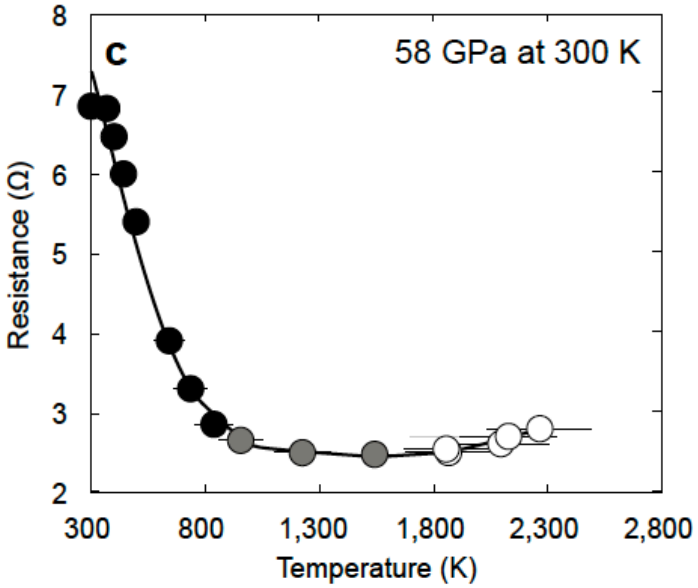

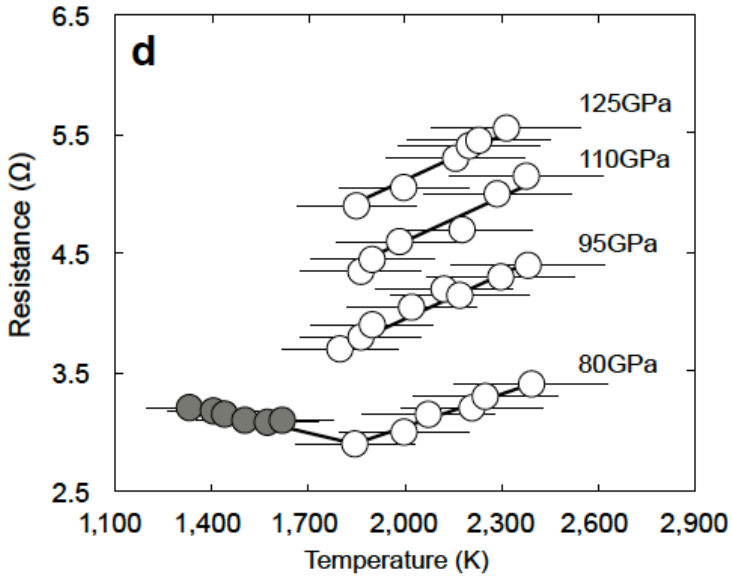

Ohta, Cohen, et al., 2012

Kenji Ohta, Katsuya Shimizu, Osaka University, Yasuo Ohishi, Japan Synchrotron Radiation Research Institute, Kei Hirose, Tokyo Institute of Technology

FeO d dos (Maximum entropy)

e_g

t_{2g}

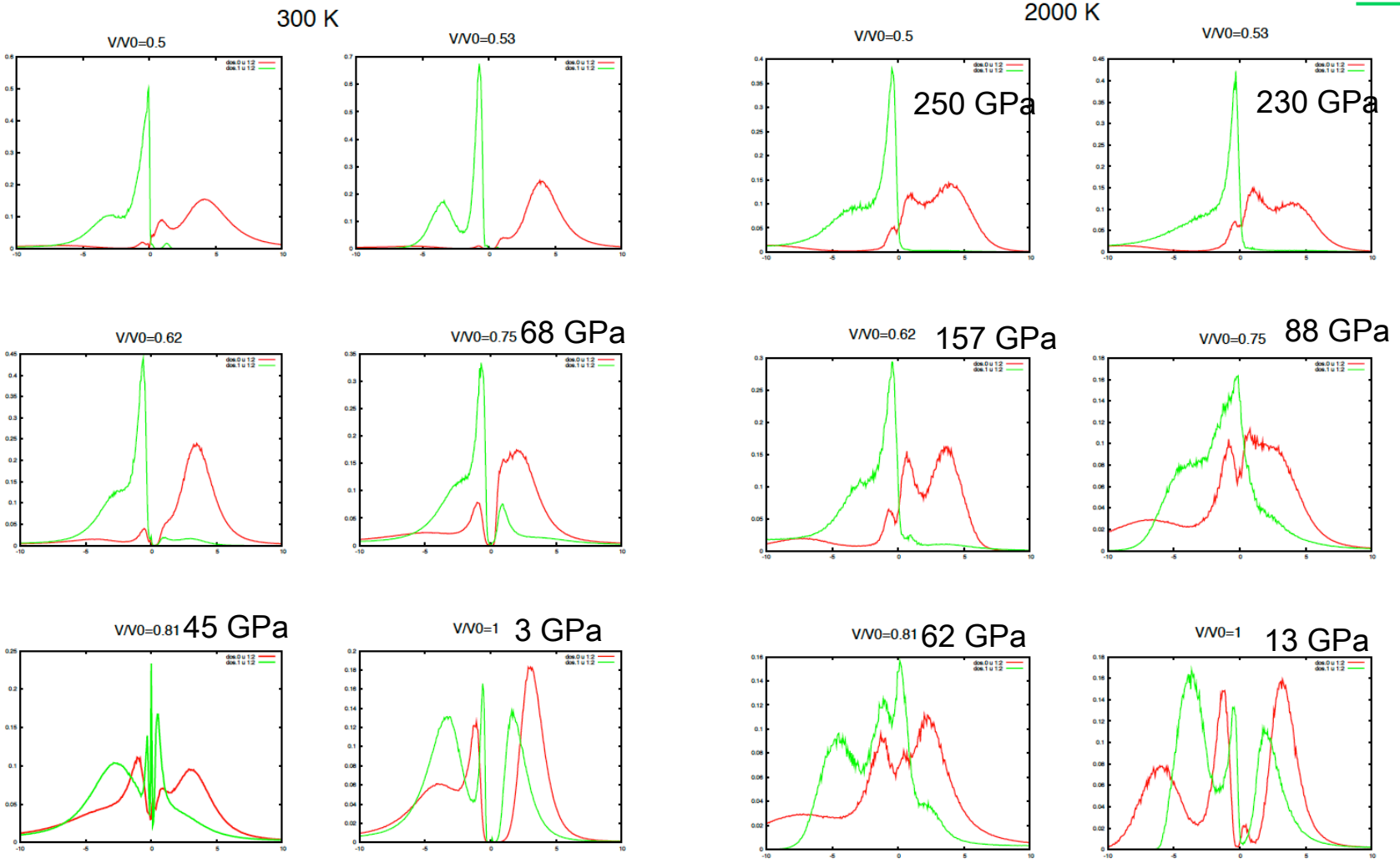

FeO Density of States

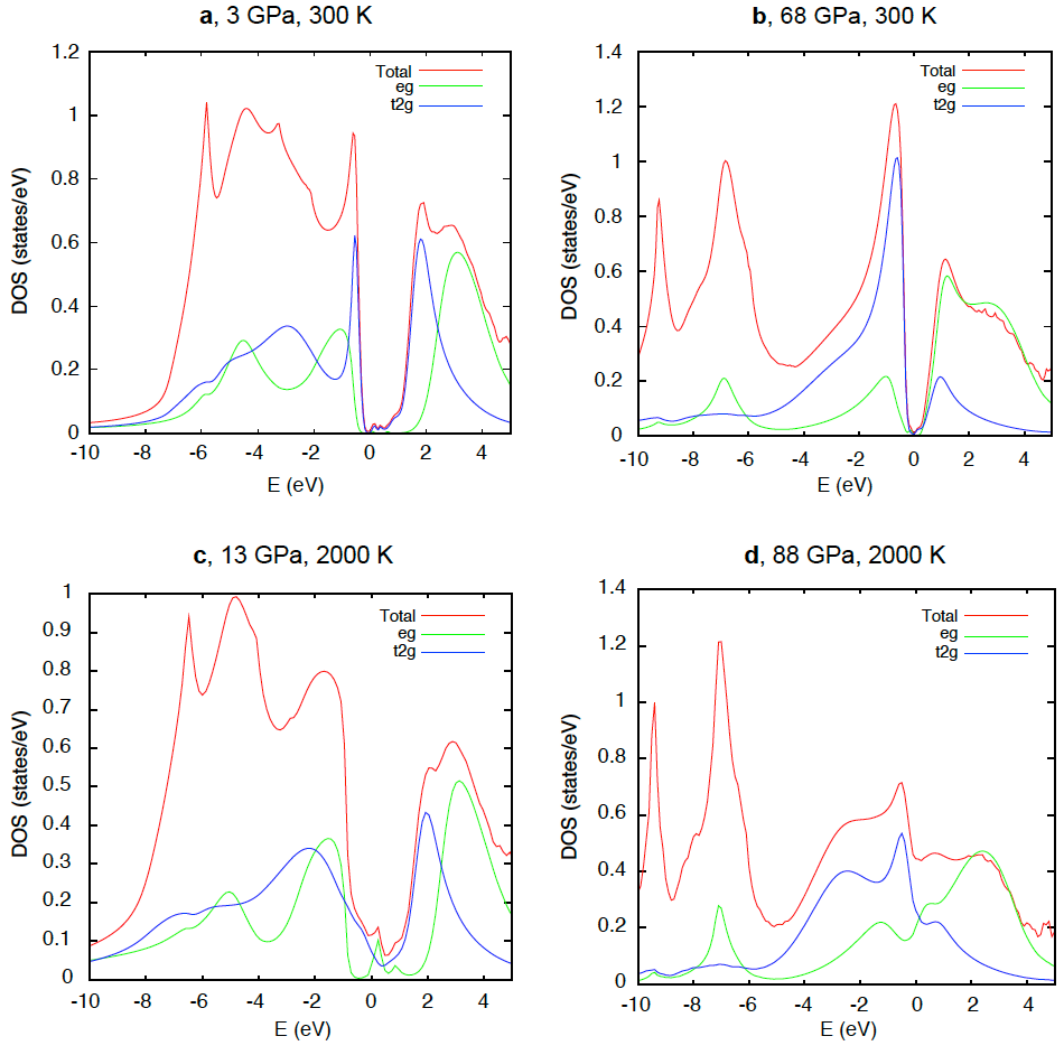

Ohta et al., 2011

Experimental and Theoretical Evidence for Pressure-Induced Metallization in FeO with Rocksalt-Type Structure

Kenji Ohta,[1,*] R. E. Cohen,[2,*] Kei Hirose,[3,4] Kristjan Haule,[5] Katsuya Shimizu,[1] and Yasuo Ohishi[6]

DC conductivity versus pressure

$$\mathrm{Im}\,\chi_{\mu\nu}(\omega) = \frac{\pi e_0^2}{V_0}\sum_{\mathbf{k}}\int dy[f(y-\omega)-f(y)] \times \mathrm{Tr}[\rho_{\mathbf{k}}(y)v^{\mathbf{k}\mu}\rho_{\mathbf{k}}(y-\omega)v^{\mathbf{k}\nu}],$$

$$\rho_{\mathbf{k}} = (G^{\dagger}-G)/(2\pi i)$$

$$\sigma'^{\mu\nu} = \frac{\pi e_0^2}{V_0}\sum_{\mathbf{k}}\int dy\left(-\frac{df}{dy}\right)\mathrm{Tr}[\rho_{\mathbf{k}}(y)v^{\mathbf{k}\mu}\rho_{\mathbf{k}}(y)v^{\mathbf{k}\nu}].$$

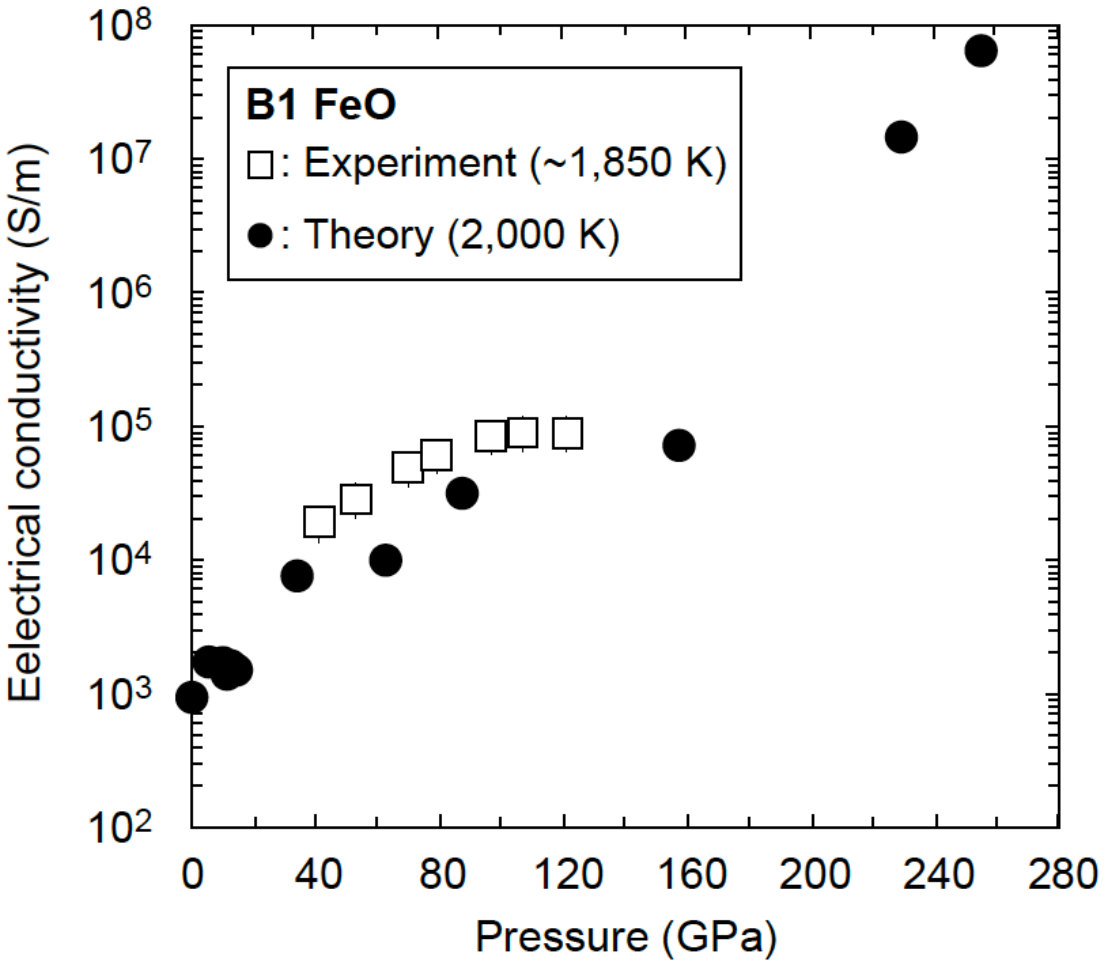

Metallization is not like this in FeO:

Magnetic state, complex phase diagrams, transitions with large density and elasticity changes, T-dependent electronic structure, sensitivity to defects, chemistry and strain (stress) state, metal-insulator transitions

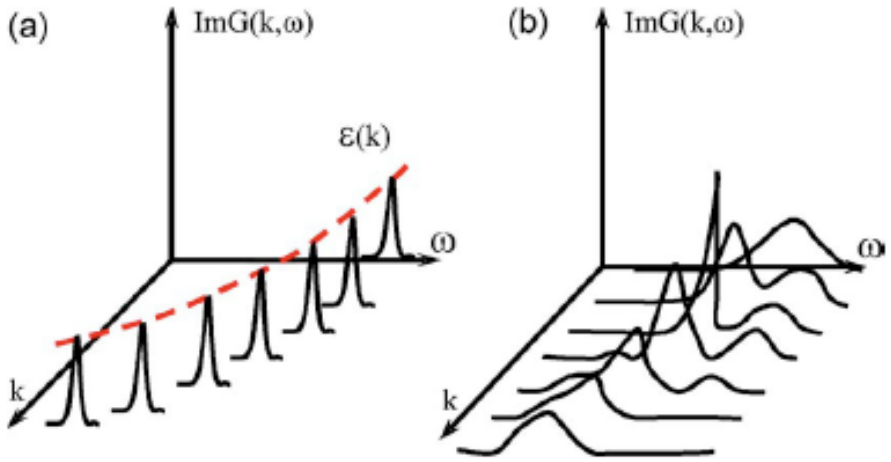

FIG. 1. (Color online) Examples of a spectrum (a) for a weakly correlated system and (b) for a strongly correlated system. The situation in (a) can be modeled by the Kohn-Sham spectra of LDA-like treatments while the description of (b) requires a many-body treatment such as DMFT.

Kotliar et al. RMP (2006)

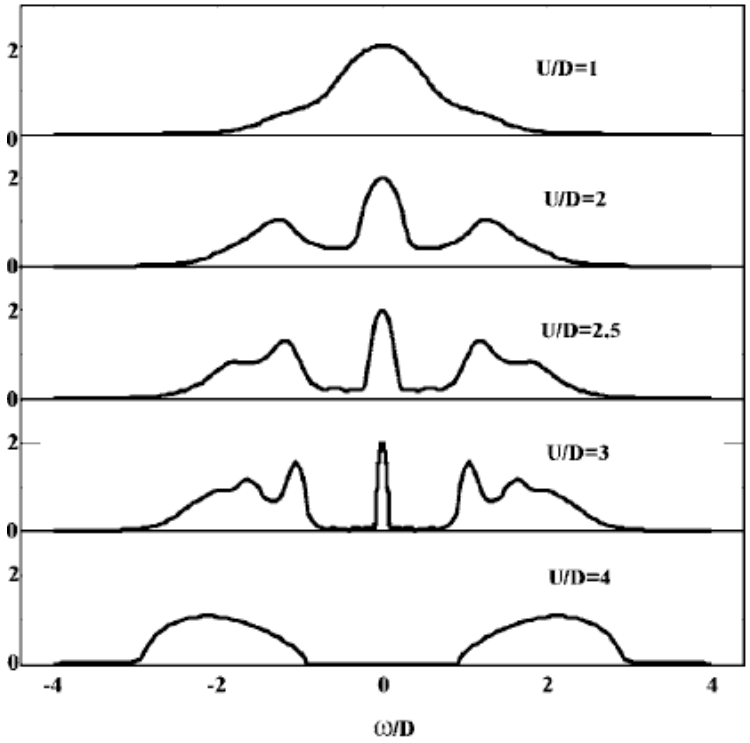

Metal insulator transition (Hubbard model)

DMFT orbital occupancy transition (HS-LS crossover)

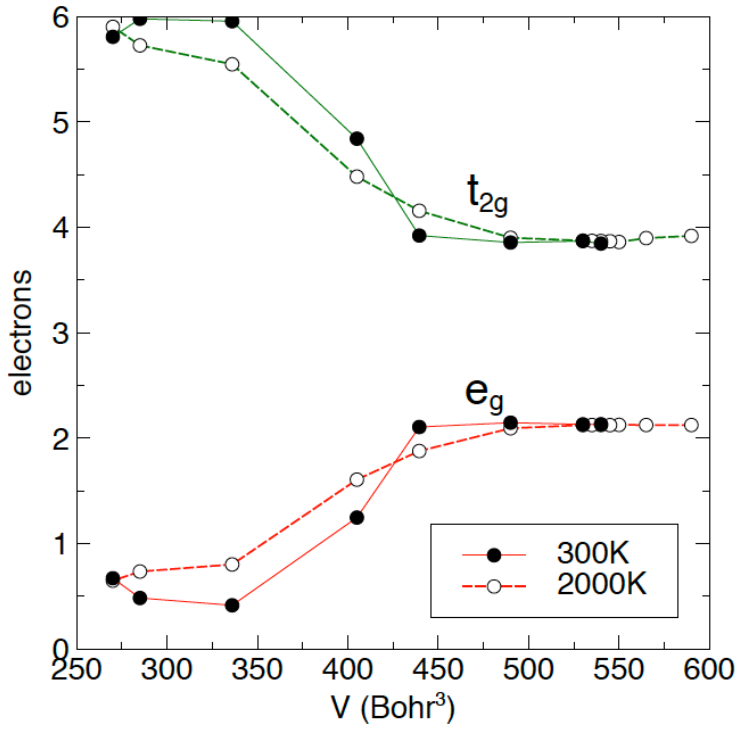

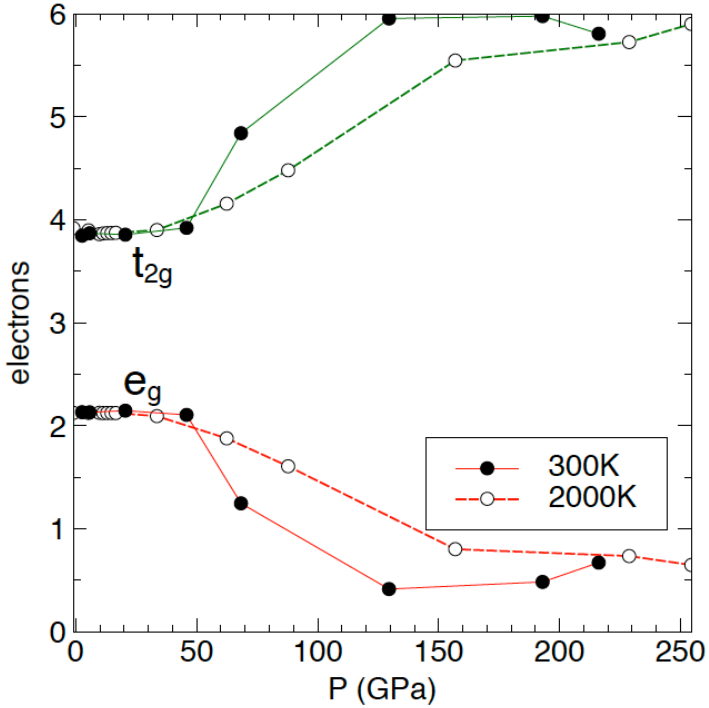

Experimental equation of state:
Fischer et al. EPSL 2011

Spectral Function A(k,ω)

V=405 au, V/V0=0.75, 68 GPa 300K

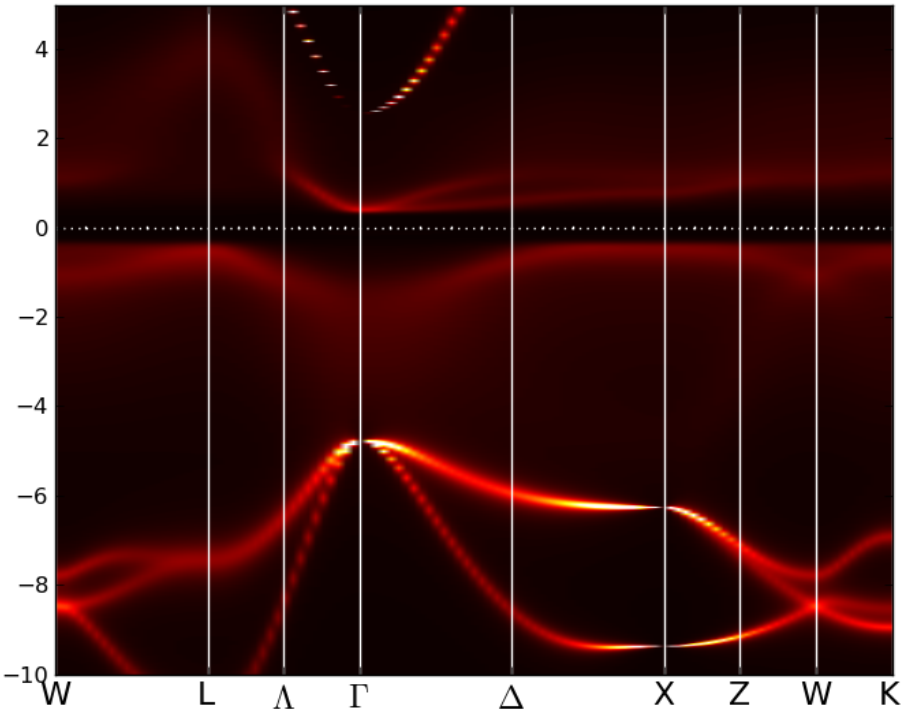

V=405 au, V/V0=0.75, 88 GPa 2000K

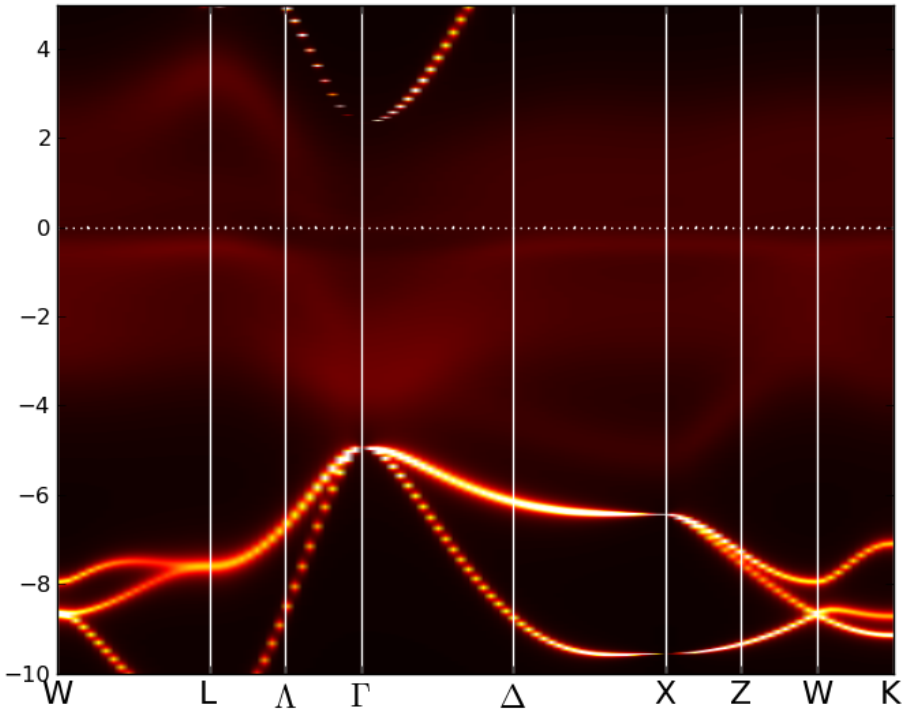

Low spin insulator -> low spin metal

High spin at low P

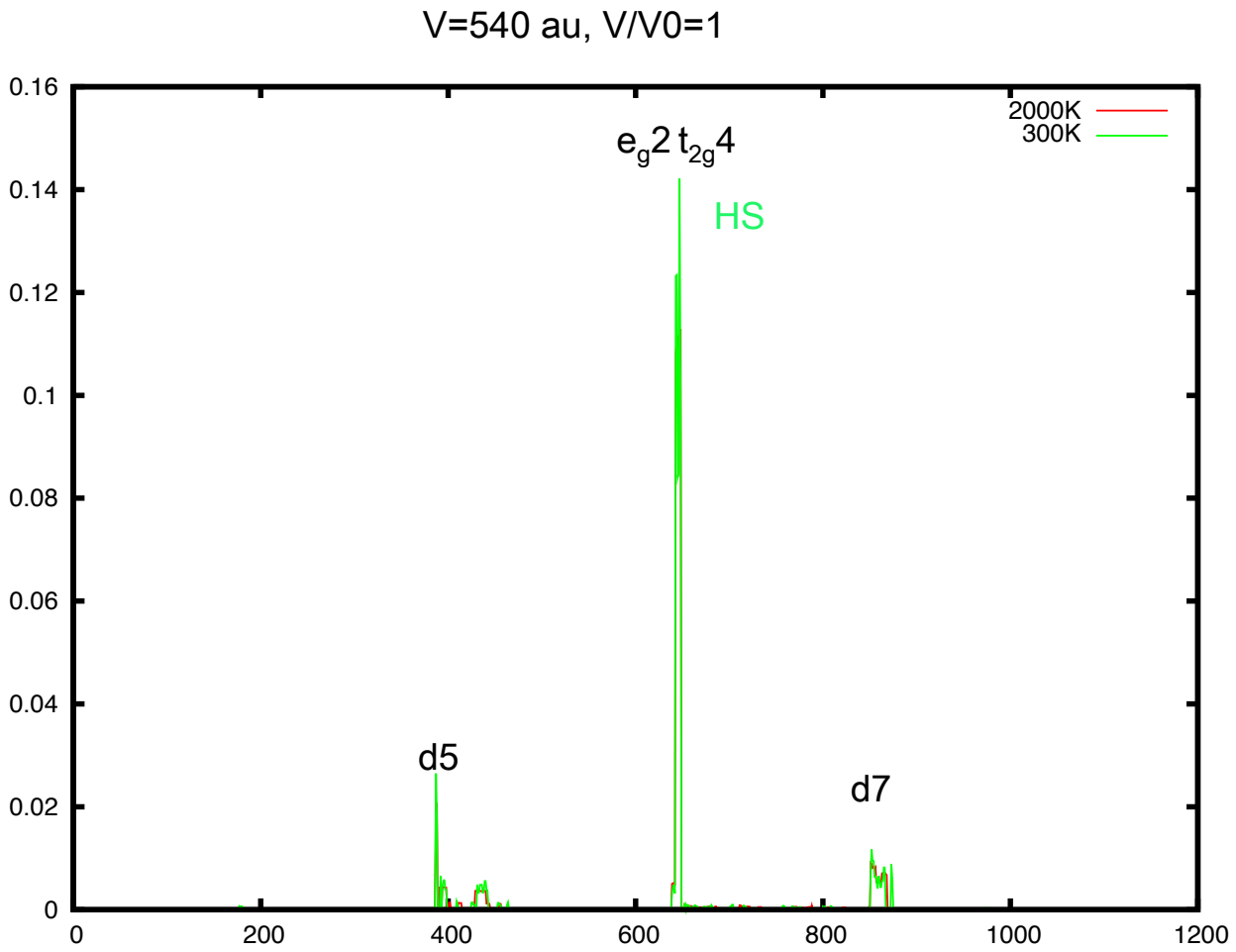

Spin fluctuations ➔ metallization

V=405 au, V/V0=0.75, 68 GPa 300K

V=405 au, V/V0=0.75, 88 GPa 2000K

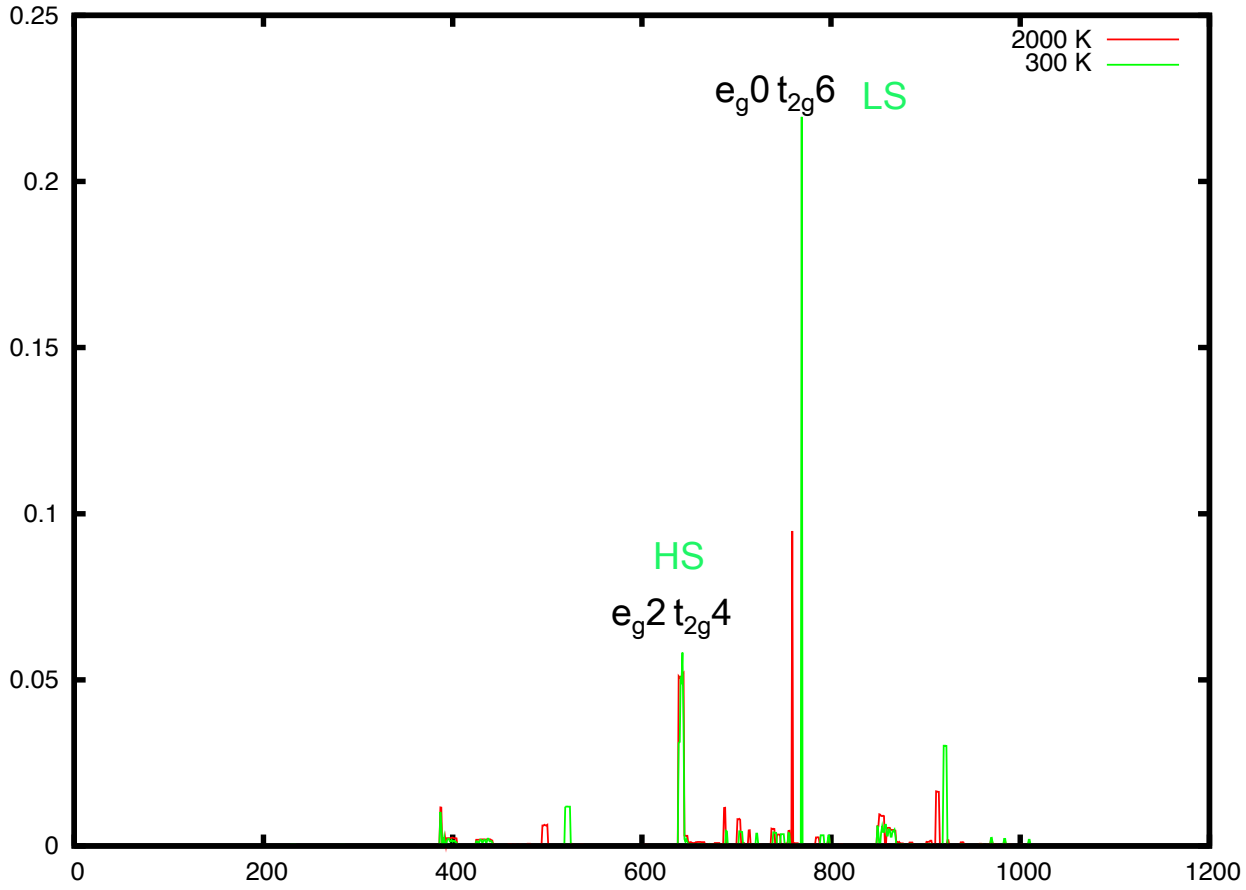

More could be said…

- SiO_2 (CASINO) (Driver, Cohen, Wu, Militzer, Rios, Towler, Needs, & Wilkins, *PNAS* **107**, 9519 (2010).
- qmcpack on GPUs (Esler, Kim, Ceperley)
- c-BN (qmcpack, GPU)(Esler, Cohen, Militzer, Kim, Needs, & Towler, PRL **104**, 185702 (2010).
- $MgSiO_3$ (qmcpack, GPU) (Lin et al., submitted)
- $FeSiO_3$ (DFT, xtalopt)(Cohen and Lin, submitted)
- FeO (DFT-DMFT) (Ohta, Cohen, Hirose, Haule, Shimizu & Ohishi, PRL**108**, 026403, (2012)—now χ and T_N with Peng Zhang